Cell Research (2011) 21:1487-1508.

www.nature.com/cr

ORIGINAL ARTICLE

HDAC2 phosphorylation-dependent Klf5 deacetylation and RARα acetylation induced by RAR agonist switch the transcription regulatory programs of *p21* in VSMCs

Bin Zheng[1], Mei Han[1], Ya-nan Shu[1], Ying-jie Li[1], Sui-bing Miao[1], Xin-hua Zhang[1], Hui-jing Shi[1], Tian Zhang[1], Jin-kun Wen[1]

[1]*Department of Biochemistry and Molecular Biology, Key Laboratory of Neural and Vascular Biology, Ministry of Education, Hebei Medical University, No. 361, Zhongshan East Road, Shijiazhuang 050017, China*

Abnormal proliferation of vascular smooth muscle cells (VSMCs) occurs in hypertension, atherosclerosis and restenosis after angioplasty, leading to pathophysiological vascular remodeling. As an important growth arrest gene, *p21* plays critical roles in vascular remodeling. Regulation of p21 expression by retinoic acid receptor (RAR) and its ligand has important implications for control of pathological vascular remodeling. Nevertheless, the mechanism of RAR-mediated p21 expression in VSMCs remains poorly understood. Here, we show that, under basal conditions, RARα forms a complex with histone deacetylase 2 (HDAC2) and Krüppel-like factor 5 (Klf5) at the *p21* promoter to inhibit its expression. Upon RARα agonist stimulation, HDAC2 is phosphorylated by CK2α. Phosphorylation of HDAC2, on the one hand, promotes its dissociation from RARα, thus allowing the liganded-RARα to interact with co-activators; on the other hand, it increases its interaction with Klf5, thus leading to deacetylation of Klf5. Deacetylation of Klf5 facilitates its dissociation from the *p21* promoter, relieving its repressive effect on the *p21* promoter. Interference with HDAC2 phosphorylation by either CK2α knockdown or the use of phosphorylation-deficient mutant of HDAC2 prevents the dissociation of Klf5 from the *p21* promoter and impairs RAR agonist-induced *p21* activation. Our results reveal a novel mechanism involving a phosphorylation-deacetylation cascade that functions to remove the basal repression complex from the *p21* promoter upon RAR agonist treatment, allowing for optimum agonist-induced p21 expression.

***Keywords*:** vascular smooth muscle cells; Krüppel-like factor 5; retinoic acid receptor α; p21; gene expression; signal transduction

Cell Research (2011) **21**:1487-1508. doi:10.1038/cr.2011.34; published online 8 March 2011

Introduction

Abnormal proliferation of vascular smooth muscle cells (VSMCs) causes intimal thickening of the vessel wall, which is strongly related to the development of atherosclerosis, restenosis and hypertension [1, 2]. Cell proliferation is coupled with cell cycle progression, promoted by cyclins (e.g., cyclin D1, cyclin E and cyclin A) and inhibited by cyclin-dependent kinase inhibitors (CKIs, e.g., p21 and p27) [3]. Among them, p21 plays critical roles in various biological processes, such as cell cycle control, DNA repair, antiapoptosis, differentiation and tumor suppression [4-7]. In the vascular system, p21 can block SMC proliferation *in vitro* and decrease restenosis in the rat model of carotid injury [8]. Recent results revealed that mice with homozygous deletion of *p21* displayed accelerated proliferations of VSMCs and enhanced neointimal formation following arterial injury [9, 10]. As an important growth arrest gene, regulation

Correspondence: Jin-kun Wen
Tel: +86-311-86265563; Fax: +86-311-86266180
E-mail: wjk@hebmu.edu.cn

Abbreviations: VSMCs (vascular smooth muscle cells); Klf5 (Krüppel-like factor 5); RARα (retinoic acid receptor α); HDAC2 (histone deacetylase 2); p21 (p21WAF1/CIP1); Cdks (cyclin-dependent kinases); ATRA (all-*trans* retinoic acid); TCE (Klf5-binding sites); RARE (RARα-binding sites); CK2 (casein kinase II); PCNA (proliferating cell nuclear antigen)

Received 30 August 2010; revised 19 December 2010; accepted 10 January 2011; published online 8 March 2011

of p21 expression has been studied extensively, especially in tumor cells. *p21* gene is shown to be regulated by p53, signal transducer and activator of transcription 1 (STAT1), retinoic acid receptor (RAR)/retinoid X receptor (RXR) complex, krüppel-like factors (Klfs), AP1, cAMP response element-binding protein (CREB), SP1, E2F and ubiquitin-like with PHD and RING finger domains 1 (UHRF1), etc. [11-20]. However, the mechanism controlling p21 expression in VSMCs is still poorly understood. In VSMCs, p21, at low levels, has growth-permissive effects by promoting the Cdk:cyclin complex formation, but a higher level of p21 has growth-inhibitory effects [21]. Recent studies have indicated that transcription factors p53, Klfs and RARs all participate in the transcription regulation of *p21* in VSMCs [14, 19, 22]. For example, retinoids could activate the expression of p21 through the RAR/RXR heterodimer [14]. We have found that angiotensin II could stimulate krüppel-like factor 5 (Klf5, also known as intestine-enriched krüppel-like factor or IKLF) phosphorylation and its interaction with c-Jun, which suppresses the expression of p21 [23]. Krüppel-like factor 4 (GKLF, Klf4) interacts with p53, and inhibits VSMC proliferation by promoting the expression of p21 [24]. Interestingly, among the factors that are known to regulate p21 expression, RARα and Klf5 could interact with each other and appear to have opposite regulatory effects on VSMC proliferation [25].

Klf5, a zinc finger-containing transcription factor, interacts with many other transcription factors, such as c-Jun, RARα, CREB binding protein (CBP) and PPAR-δ, and regulates the expression of many genes involved in cell proliferation [26]. RARs belong to the nuclear receptor superfamily, and when bound by their ligands, such as Am80 or AtRA, promote VSMC differentiation [27-29]. As a result, RAR is now considered to be an attractive target for treatment of VSMC proliferation diseases [30, 31]. Generally, in the absence of ligands, RARs are associated with co-repressors to inhibit transcription, while liganded RARs recruit co-activators to activate transcription [32]. Clinical applications of AtRA have had some success in the treatment of human diseases such as cancer, psoriasis, leukemia, restenosis and plaque formation [31, 33]. Nevertheless, the precise mechanism by which RARs function to control *p21* and thus govern cell proliferation is still not well understood.

In this study, using the VSMC model system, we show that RARα forms a complex with HDAC2 and Klf5 at the *p21* promoter to inhibit its expression under basal conditions. Interestingly, RAR agonist treatment leads to CK2α-mediated phosphorylation of HDAC2. Phosphorylation of HDAC2 switches its interaction preference from RAR to Klf5, and thus promotes Klf5 deacetylation. Deacetylated Klf5 then dissociates from the *p21* promoter, and the consequent loss of Klf5-mediated repression further facilitates RAR agonist-stimulated p21 expression. Our study reveals novel mechanistic insights of RAR-mediated regulation of p21 expression.

Results

Klf5 and RARα cooperatively inhibit the transcription of p21 under basal conditions

The promoter region of *p21* contains both RARα-binding sites and *cis*-elements for Klfs [14, 23]; moreover, RARα is shown to interact with Klf5 [25, 34]. To gain further insights into their roles in p21 expression, VSMCs were either infected with an adenovirus vector expressing Klf5 and RARα, or treated with siRNA against Klf5 (Klf5 siRNA) or RARα (RARα siRNA). First, we identified that siRNAs targeting Klf5 and RARα were highly specific for VSMCs, that is, Klf5 siRNA knocked down Klf5 expression but had no effect on RARα expression, and RARα siRNA knocked down RARα expression but had no effect on RARβ expression (Supplementary information, Figure S1). Silencing RARα or Klf5 by specific siRNA increased p21 expression by 2.64-fold and 1.98-fold, respectively (Figure 1A). In contrast, overexpression of Klf5 and RARα attenuated p21 expression by 68% and 59%, respectively, and co-infection of Klf5 and RARα resulted in an almost complete inhibition of p21 expression (Figure 1B). These results clearly suggest that Klf5 and RARα cooperatively inhibit the expression of p21. Similarly, when the expression vectors for Klf5 or RARα were cotransfected into 293A cells along with the *p21* promoter reporter, the overexpression of Klf5 or RARα decreased the reporter activity by 62% and 57%, respectively, compared with the reporter alone. Furthermore, cotransfection of Klf5 and RARα reduced the *p21* promoter activity to 16% of the control (Figure 1C). There are four tandem typical Klf5-binding sites (TCE) and two RARα-binding sites (RARE) in the promoter region of *p21* (Figure 1D). We mutated the tandem TCE sites or the proximal RARE sites and examined which element contributed to the repression of *p21* by Klf5 or RARα. As shown in Figure 1E, mutation of TCE sites removed the inhibitory effect of Klf5, but not RARα. Likewise, mutation of RARE site removed the inhibitory effect of RARα, but not Klf5, which prompts us to speculate that the inhibitory effect of Klf5 and RARα on the *p21* promoter is relatively independent. But how do these two factors interact with each other and have the cooperatively inhibitory effect on p21 expression? When these sites were mutated simultaneously, the *p21* promoter activity increased by 17.2-

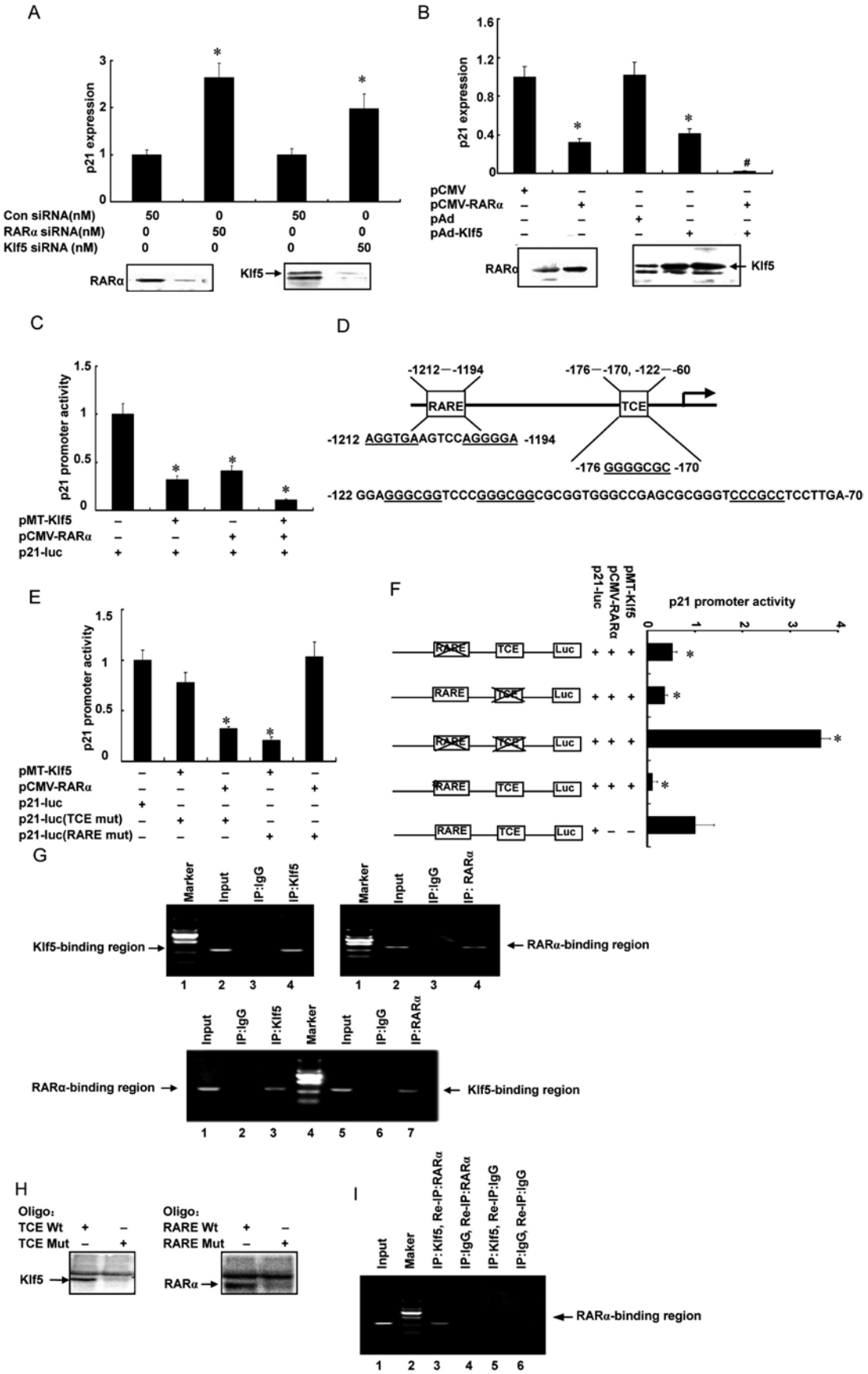
A
p21 expression
Con siRNA(nM) 50 0 50 0
RARα siRNA(nM) 0 50 0 0
Klf5 siRNA (nM) 0 0 0 50
RARα
Klf5
B
p21 expression
pCMV
pCMV-RARα
pAd
pAd-Klf5
RARα
Klf5
C
p21 promoter activity
pMT-Klf5
pCMV-RARα
p21-luc
D
-1212—-1194
-176—-170, -122—-60
RARE
TCE
-1212 AGGTGAAGTCCAGGGGA -1194
-176 GGGGCGC -170
-122 GGAGGGCGGTCCCGGGCGGCGCGGTGGGCCGAGCGCGGGTCCCGCCTCCTTGA-70
E
p21 promoter activity
pMT-Klf5
pCMV-RARα
p21-luc
p21-luc(TCE mut)
p21-luc(RARE mut)
F
p21 promoter activity
p21-luc
pCMV-RARα
pMT-Klf5
RARE
TCE
Luc
G
Marker
Input
IP:IgG
IP:Klf5
IP: RARα
Klf5-binding region
RARα-binding region
IP:RARα
H
Oligo:
TCE Wt
TCE Mut
RARE Wt
RARE Mut
Klf5
RARα
I
Input
Maker
IP:Klf5, Re-IP:RARα
IP:IgG, Re-IP:RARα
IP:Klf5, Re-IP:IgG
IP:IgG, Re-IP:IgG
RARα-binding region

Figure 1 Klf5 and RARα cooperatively inhibit the transcription of *p21*. **(A)** VSMCs were transfected with control siRNA, Klf5 siRNA or RARα siRNA for 2 days before lysis and processed for real time RT-PCR. Bars represent means ± S.E.M. of three independent experiments. **P* < 0.05. Expression of RARα and Klf5 was assessed by western blot analysis. **(B)** VSMCs were infected with pCMV, pCMV-RARα, pAd or pAd-Klf5 for 2 days before lysis and processed for real-time RT-PCR. Bars represent means ± S.E.M. of three independent experiments. **P* < 0.05. Expression of RARα and Klf5 was assessed by western blot analysis. **(C)** 293A cells were transiently cotransfected with the 5′ regulatory region of *p21* fused to the pGL3-Basic luciferase reporter vector together with either pMT-Klf5 or pCMV-RARα. 48 h later, cells were harvested, and the activity of firefly luciferase was measured and normalized to that of Renilla luciferase. Bars represent the means ± S.E.M. from three independent experiments. **P* < 0.05. **(D)** Partial sequence of the human *p21* promoter between nucleotides −1 212 to −60. The underlined sequences are Klf5-binding sites. **(E)** 293A cells were cotransfected with *p21* wild-type or RARE- and TCE-mutated promoter-reporter constructs together with pMT-Klf5 and pCMV-RARα. 24 h later, luciferase activity was measured as indicated above. Bars represent the means ± S.E.M. of three independent experiments. **P* < 0.05. **(F)** The mutations of RARE site and TCE sites on the *p21* promoter region are schematically represented on the left of the figure. 293A cells were cotransfected with these *p21* promoter-reporter constructs together with pMT-Klf5 and pCMV-RARα. 24 h later, luciferase activity was measured as indicated above. Bars represent the means ± S.E.M. of three independent experiments. **P* < 0.05. **(G)** Chromatin immunoprecipitation was performed using anti-Klf5 (left panel) and anti-RARα (right panel) antibodies. The PCR was performed using Klf5 (left panel) and RARα-binding region-specific primers (right panel). Chromatin fragment was also immunoprecipitated using anti-Klf5 or anti-RARα antibodies and amplified by RARα- (lanes 1-3) or Klf5 (lanes 5-7)-binding region-specific primers (lower panel), respectively. Non-immune IgG was used as negative control for immunoprecipitation, water as the PCR negative control, and input corresponds to extracted DNA from the sample prior to immunoprecipitation. The results are from representative experiments that have been repeated 3 times with similar results. **(H)** VSMCs were lysed. The lysates were precleared with ImmunoPure streptavidin-agarose beads (20 μl/sample) for 1 h, and incubated with 100 pmol of biotinylated double-strand oligonucleotides for Klf5-binding sites (including three tandem TCE sites together, RARE WT or its mutant RARE Mut) or RARα-binding sites (including two proximal RARE sites together) and 10 μg of poly (dI-dC)·poly (dI-dC) for 16 h. DNA-bound proteins were collected with 30 μl immobilized streptavidin-agarose beads for 1 h, and subjected to western blotting with anti-Klf5 or anti-RARα antibodies. **(I)** Chromatin fragments were immunoprecipitated with anti-Klf5 antibody, followed by a brief treatment with 0.5% SDS-containing buffer. The released material was then subjected to a second immunoprecipitation with anti-RARα antibody. Immunoprecipitated DNA was amplified by PCR using RARα-binding region specific primers. IgG as a negative control for the first or/and secondary ChIP assay.

fold compared with the wild-type promoter (Figure 1F). These data suggest that Klf5 and RARα exert a synergistic inhibitory effect on the transcription of *p21*. To test whether the *p21* promoter is a direct target for Klf5 and RARα, chromatin immunoprecipitation (ChIP) was performed. As shown in Figure 1G, both the Klf5-binding region and the RARα-binding region could be amplified by PCR using two sets of primers specific for these two regions. Moreover, Klf5 was also detected in RARα immunoprecipitates, and vice versa, suggesting that an interaction between Klf5 and RARα exists within the intact chromatin. Oligo pull-down assays showed that mutation in each of these two sequences abolished their binding to either Klf5 or RARα (Figure 1H). To further identify the interaction between Klf5 and RARα, a two-step ChIP assay was performed, in which the Klf5 immunoprecipitates were subjected to a second immunoprecipitation with anti-RARα followed by PCR amplification with the primers specific for the RARα-binding region. Under these conditions, the RARα-binding region was still specifically detected (Figure 1I). These results suggest that Klf5 forms a stable complex with RARα that is bound to the RARα-binding region of the *p21* promoter.

HDAC2 mediates the inhibitory effect of Klf5 and RARα on the transcription of p21

The above results suggest that Klf5 and RARα cooperatively inhibit the expression of p21. This finding is noteworthy because, to our knowledge, many of the genes identified to date as direct targets of Klf5 are transactivated by Klf5. So we speculate that the inhibitory effect of Klf5 on *p21* might involve its interaction with other co-repressors. To test this, we performed co-immunoprecipitation (Co-IP) and western blotting to examine the immunoprecipitates pulled down by anti-RARα and anti-Klf5 antibodies. As shown in Figure 2A, aside from Klf5 and RARα, which were detected to interact with each other, HDAC2 was detected in the two immunoprecipitates, suggesting that Klf5 and RARα form a complex with HDAC2 (Figure 2A). A two-step ChIP assay showed that both Klf5- and RARα-binding regions could be amplified in the immunoprecipitates pulled down first with anti-HDAC2 and second with anti-RARα or anti-Klf5, further supporting that an interaction between Klf5, RARα and HDAC2 exists within the intact chromatin (Figure 2B). We also used nonimmune IgG as negative control for second ChIP assays and confirmed the speci-

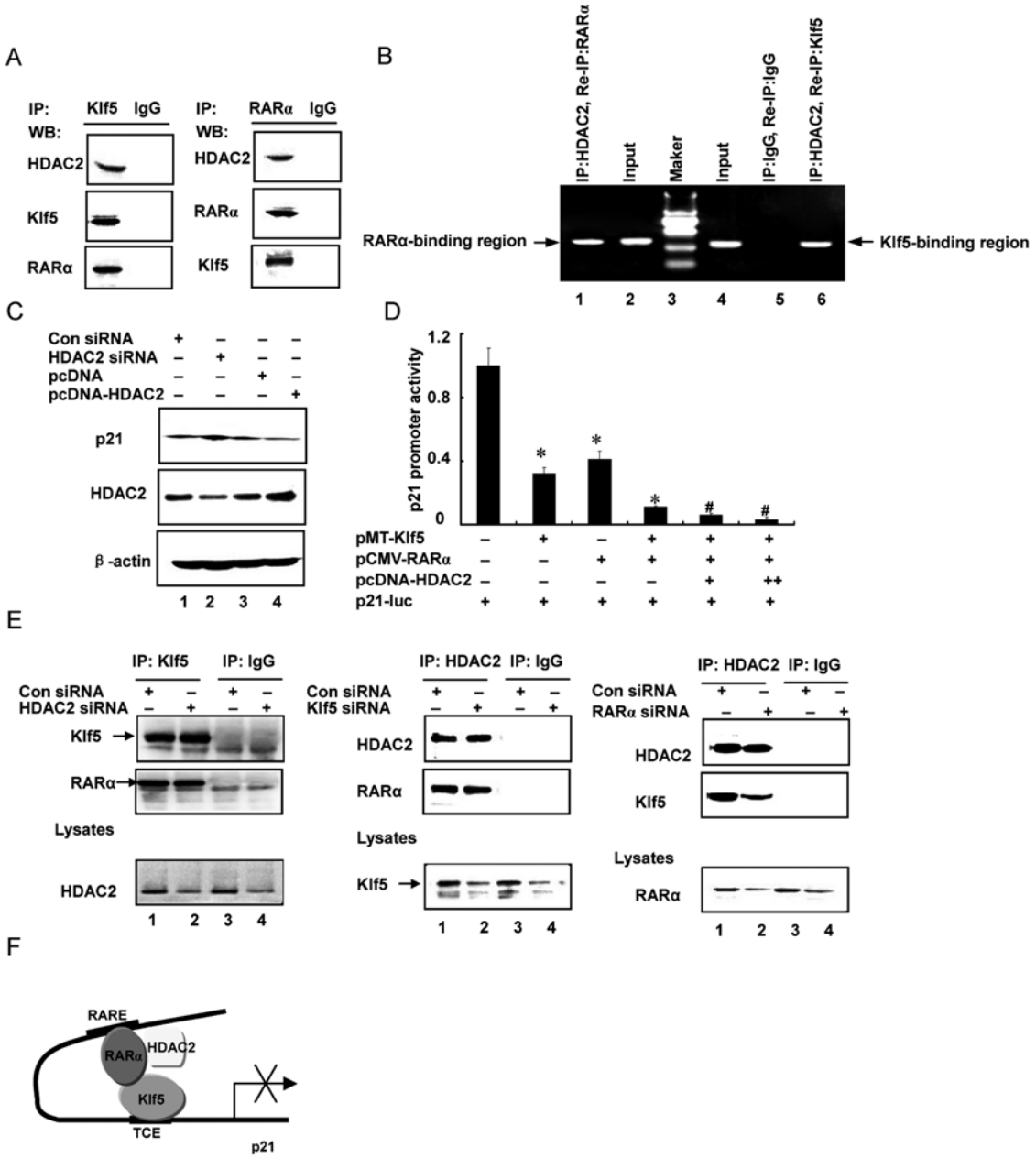

Figure 2 HDAC2 mediates the inhibitory effect of Klf5 and RARα on the transcription of *p21*. **(A)** Interaction between Klf5, RARα and HDAC2 was examined by co-immunoprecipitation (Co-IP) and western blot analysis with the indicated antibodies. Anti-Klf5 (left panel) or anti-RARα (right panel) immunoprecipitates were analyzed by western blotting with anti-HDAC2, Klf5 and RARα antibodies. **(B)** Chromatin fragments were immunoprecipitated with anti-HDAC2 antibody, followed by a brief treatment with 0.5% SDS-containing buffer. The released material was then subjected to a second immunoprecipitation with anti-RARα or anti-Klf5 antibodies. Immunoprecipitated DNA was amplified by PCR using RARα-(lanes 1-3) or Klf5 (lanes 5-7)-binding region-specific primers. IgG was used as a negative control. **(C)** VSMCs were transfected with control siRNA, HDAC2 siRNA and pcDNA-HDAC2 for 48 h before lysis and processed for western blotting with anti-p21 and anti-HDAC2 antibodies. **(D)** 293A cells were transiently cotransfected with the *p21*-reporter constructs together with pMT-Klf5, pCMV-RARα or pcDNA-HDAC2. 48 h later, cells were harvested, and the activity of firefly luciferase was measured and normalized to that of Renilla luciferase. Bars represent the means ± S.E.M. from three independent experiments. **P* < 0.05. **(E)** VSMCs were transfected with control siRNA, HDAC2 siRNA (left panel), Klf5 siRNA (middle panel), or RARα siRNA (right panel) for 48 h before lysis. Total protein lysates were collected and immunoprecipitated with the indicated antibodies. Immunoprecipitates were analyzed by western blotting with the indicated antibodies. **(F)** Model of the transcriptional repression complex formed by RARα, Klf5 and HDAC2 on the *p21* promoter.

ficity of immunoprecipitation (Supplementary information, Figure S2). We next examined the effect of HDAC2 on p21 expression. As shown in Figure 2C, transfection of pcDNA-HDAC2 into VSMCs resulted in a decrease in p21 expression. Conversely, depletion of endogenous HDAC2 by HDAC2-specific siRNA led to an increase in p21 expression, suggesting that Klf5 and RARα likely form a transcriptional repression complex with HDAC2. Luciferase reporter assay showed that cotransfection of expression vectors for Klf5, RARα and HDAC2 into 293A cells markedly attenuated the *p21* promoter activity compared with co-expression of Klf5 and RARα only (Figure 2D), again indicating that HDAC2 is involved in the synergistic inhibition of the *p21* promoter by Klf5 and RARα. We further determined how Klf5 and RARα interact with HDAC2. We found that knockdown of HDAC2 did not affect the interaction between Klf5 and RARα (Figure 2E, left panel); knockdown of Klf5 also did not change the association of HDAC2 with RARα (Figure 2E, middle panel). However, when RARα was knocked down, the interaction between HDAC2 and Klf5 was significantly reduced (Figure 2E, right panel). These data suggest that HDAC2 interacts with RARα directly, while its interaction with Klf5 is indirect and mediated by RARα (Figure 2F).

Am80 reverses the inhibitory effect of Klf5 and RARα on the transcription of p21 by disrupting the Klf5-RARα-HDAC2 repression complex

It is known that, as a RARα-specific agonist, Am80 inhibits phenotypic modulation and proliferation of VSMCs [34]. We next examined the effect of Am80 on p21 expression. Immunoblotting showed that Am80 upregulated p21 expression in a dose-dependent manner (Figure 3A, upper panel). Ro 41-5253, a RARα-specific antagonist, could block Am80-induced expression of p21 (Figure 3A, lower panel). Luciferase reporter assay showed that Am80 increased the *p21* promoter activity in a concentration-dependent fashion (Figure 3B). To test whether Am80-induced expression of p21 is related to the disruption of the Klf5-RARα-HDAC2 transcriptional repression complex, we performed a Co-IP assay and found that Am80 significantly reduced the interaction between Klf5 and RARα (Figure 3C) as well as that between HDAC2 and RARα (Figure 3D) in a dose-dependent manner. In contrast, Am80 increased the interaction of Klf5 with HDAC2 (Figure 3E). Dual immunofluorescent detection revealed that while Klf5 or RARα colocalized with HDAC2 under basal conditions, Am80 promoted the interaction between HDAC2 and Klf5, and inhibited the interaction between HDAC2 and RARα (Figure 3F and 3G), consistent with the Co-IP results. Given that Am80 disrupted the repression complex formed by Klf5, RARα and HDAC2, we tested whether Am80 affected the binding activity of Klf5 and RARα to their respective binding sites. Oligo pull-down assays showed that Am80 significantly increased the binding of RARα to the RARE site (Figure 3H, upper panel, compare lane 1 and lane 2). In contrast, the binding of Klf5 to the TCE sites was abrogated by Am80 (Figure 3H, lower panel, compare lane 1 and lane 2). We next performed ChIP assays and confirmed that Am80 increased the RARα binding to the *p21* promoter and markedly decreased the binding of Klf5 to the *p21* promoter (Figure 3I), which is consistent with the oligo pull-down data. These results suggest that Am80 treatment disrupts the Klf5-RARα-HDAC2 transcriptional repression complex at the *p21* promoter.

Am80-induced deacetylation of Klf5 facilitates its dissociation from the p21 promoter

As Am80 increased the interaction of Klf5 with HDAC2 (Figure 3E), we sought to determine whether Am80-induced interaction of Klf5 with HDAC2 affected Klf5 acetylation. Indeed, we found that Am80 decreased the level of acetylated Klf5 in a dose-dependent manner (Figure 4A). We mutated the Klf5 acetylation site (Klf5 K369R) and transfected this mutant form into 293A cells. As shown in Figure 4B, the Klf5 K369R mutant showed a reduced interaction with RARα, which is similar to the reduced interaction between wild-type Klf5 and RARα in the presence of Am80. Reporter gene assay showed that co-expression of Klf5 and p300 (a transcriptional coactivator and histone acetyltransferase) strongly suppressed the *p21* promoter activity in a dose-dependent manner, while the K369R acetylation-deficient mutant of Klf5 lost the inhibitory effect on the *p21* promoter (Figure 4C). To further establish that the acetylation and deacetylation of Klf5 affect its binding to the *p21* promoter, oligo pull-down assay was performed. When wild-type Klf5 and p300 were co-expressed, the binding of Klf5 to the TCE sites significantly increased, but when the acetylation site of Klf5 was mutated or when wild-type Klf5 and HDAC2 were co-expressed, almost no binding of Klf5 to the TCE sites was detected (Figure 4D). These results suggest that Am80-induced deacetylation of Klf5 stimulates its dissociation from the *p21* promoter.

Dissociation of Klf5 from the p21 promoter is mediated by HDAC2

To determine whether Klf5 deacetylation and dissociation from the *p21* promoter were mediated directly by HDAC2, we tested if knockdown of HDAC2 affected Klf5 binding to its site. Oligo pull-down assay showed that HDAC2 knockdown significantly inhibited Am80-

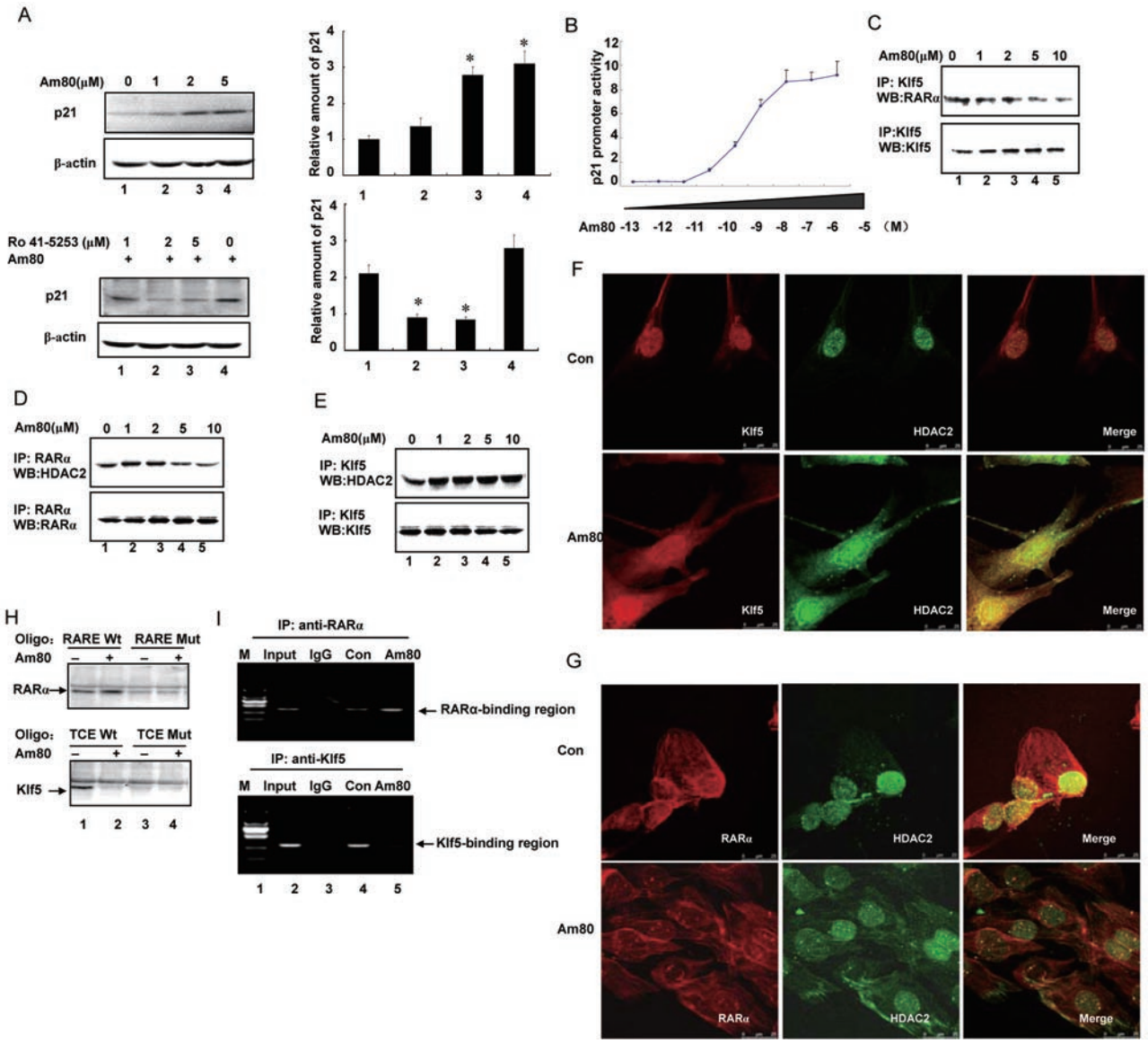

Figure 3 Am80 interrupts the interactions between Klf5, RARα and HDAC2. **(A)** VSMCs were treated with the different concentrations of Am80 (upper panel) or pretreated with Ro 41-5253 for 1 h before exposure to Am80 for 2 h (lower panel). Total protein lysates were collected and then subjected to western blotting with anti-p21 antibody. β-Actin was used as a control for equal protein loading. Left, blots from a representative experiment are shown. Right, densitometry analysis was carried out and normalized to β-actin. Bars represent the means± S.E.M. from three independent experiments **P* < 0.05. **(B)** The *p21* promoter-reporter constructs were cotransfected with pCMV-RARα into 293A cells, and cells treated with different concentrations of Am80 (10^{-13}~10^{-5} M) for 24 h. The activity of firefly luciferase was measured and normalized to that of Renilla luciferase. Bars represent the means ± S.E.M. from three independent experiments. **(C**-**E)** VSMCs were treated with different concentrations of Am80. Cell extracts were immunoprecipitated either with anti-Klf5 antibody **(C**, **E)** or with anti-RARα antibody **(D)** and immunoblotted with antibodies against RARα, Klf5 and HDAC2. **(F)** VSMCs were grown on cell culture inserts and prepared for confocal microscopy. Pictures show the same data set of cells that were simultaneously stained for HDAC2 (green), Klf5 (red) and the Merge (yellow). Magnification ×1 000. **(G)** HDAC2 (green), RARα (red), and the Merge (yellow). Pictures are single optical sections (x, y) with xz- and yz-projections, respectively. **(H)** VSMCs were treated with Am80 (2 μM) for 2 h. The lysates were subjected to oligo pull-down assay using biotinylated double-strand oligonucleotides for RARα-binding sites (upper panel) or Klf5-binding sites (lower panel). Magnification ×1 000. **(I)** VSMCs were treated with or without Am80 (2 μM) for 2 h, then crosslinked chromatin was extracted and immunoprecipitated with anti-RARα (upper panel) or anti-Klf5 (lower panel) antibodies with Am80-treated VSMCs. Non-immune IgG was used as negative control for immunoprecipitation, water as the PCR negative control, and the input corresponds to extracted DNA from the sample prior to immunoprecipitation. The results are from representative experiments that have been repeated 3 times with similar results.

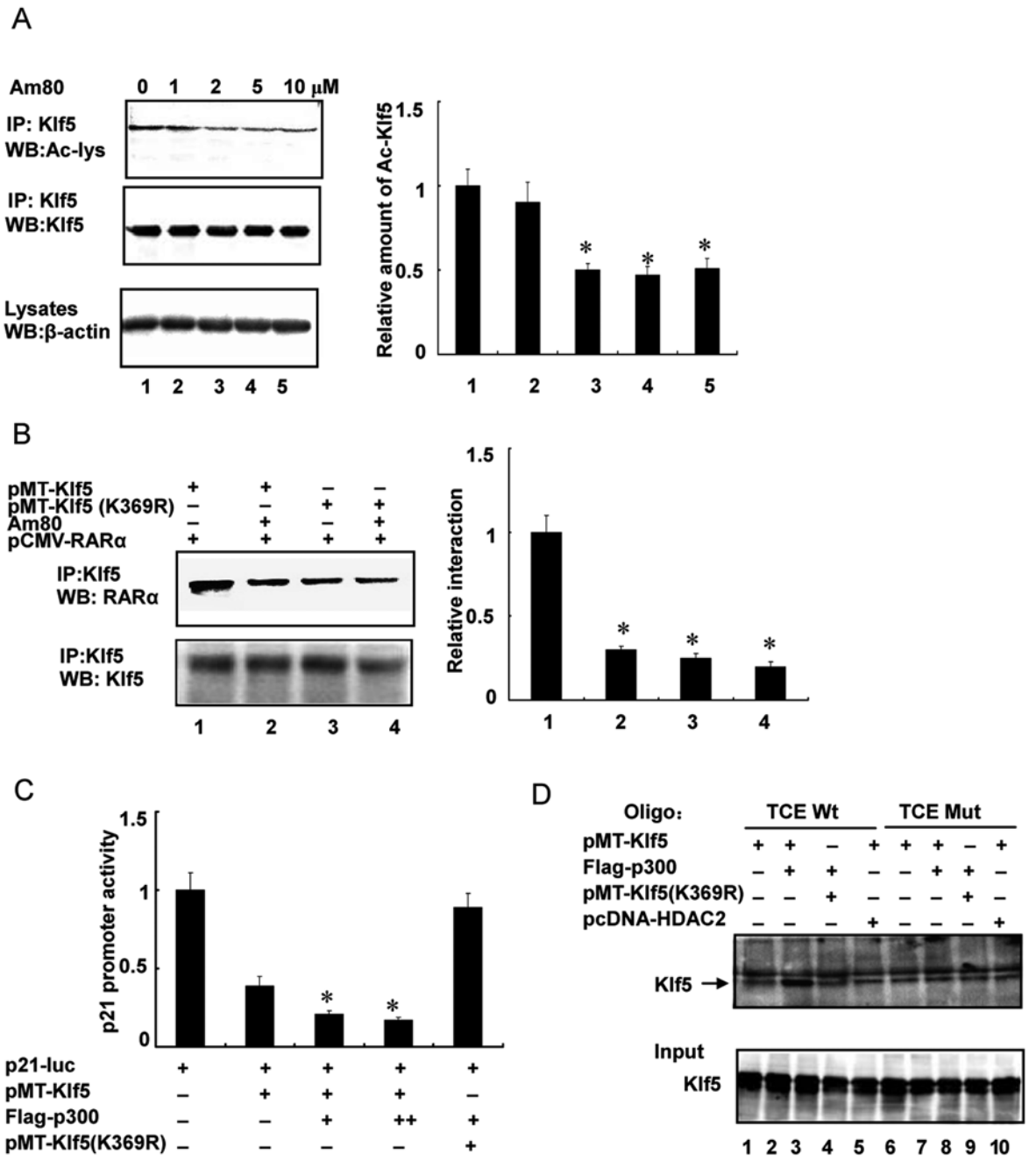

Figure 4 Am80 promotes Klf5 dissociation from the *p21* promoter. **(A)** VSMCs were treated with different concentrations of Am80. Cell extracts were immunoprecipitated with antibody against Klf5 and immunoblotted with antibody against Ac-lys or Klf5. β-Actin was used as a control for equal protein loading. Bolts from a representative experiment are shown on the left, whereas band intensities that were measured and normalized to β-actin are shown on the right. **P* < 0.05. **(B)** 293A cells were cotransfected with pMT-Klf5, pMT-Klf5 (K369R), or pCMV-RARα and treated with or without 2 μM Am80 for 2 h. Cell extracts were immunoprecipitated with antibody against Klf5 and immunoblotted with antibody against RARα or Klf5. Blots from a representative experiment are shown on the left, and band intensities of RARα are shown on the right. **P* < 0.05. **(C)** 293A cells were cotransfected with the *p21* promoter-reporter constructs, pMT-Klf5, pCMV-p300 or pMT-Klf5 (K369R). 24 h later, luciferase activity was measured as indicated above. Bars represent the means ± S.E.M. of three independent experiments. **P* < 0.05. **(D)** 293A cells were cotransfected with pMT-Klf5, pCMV-p300, pMT-Klf5 (K369R), or pcDNA-HDAC2. The lysates were subjected to oligo pull-down assay using biotinylated double-strand oligonucleotides for Klf5-binding sites.

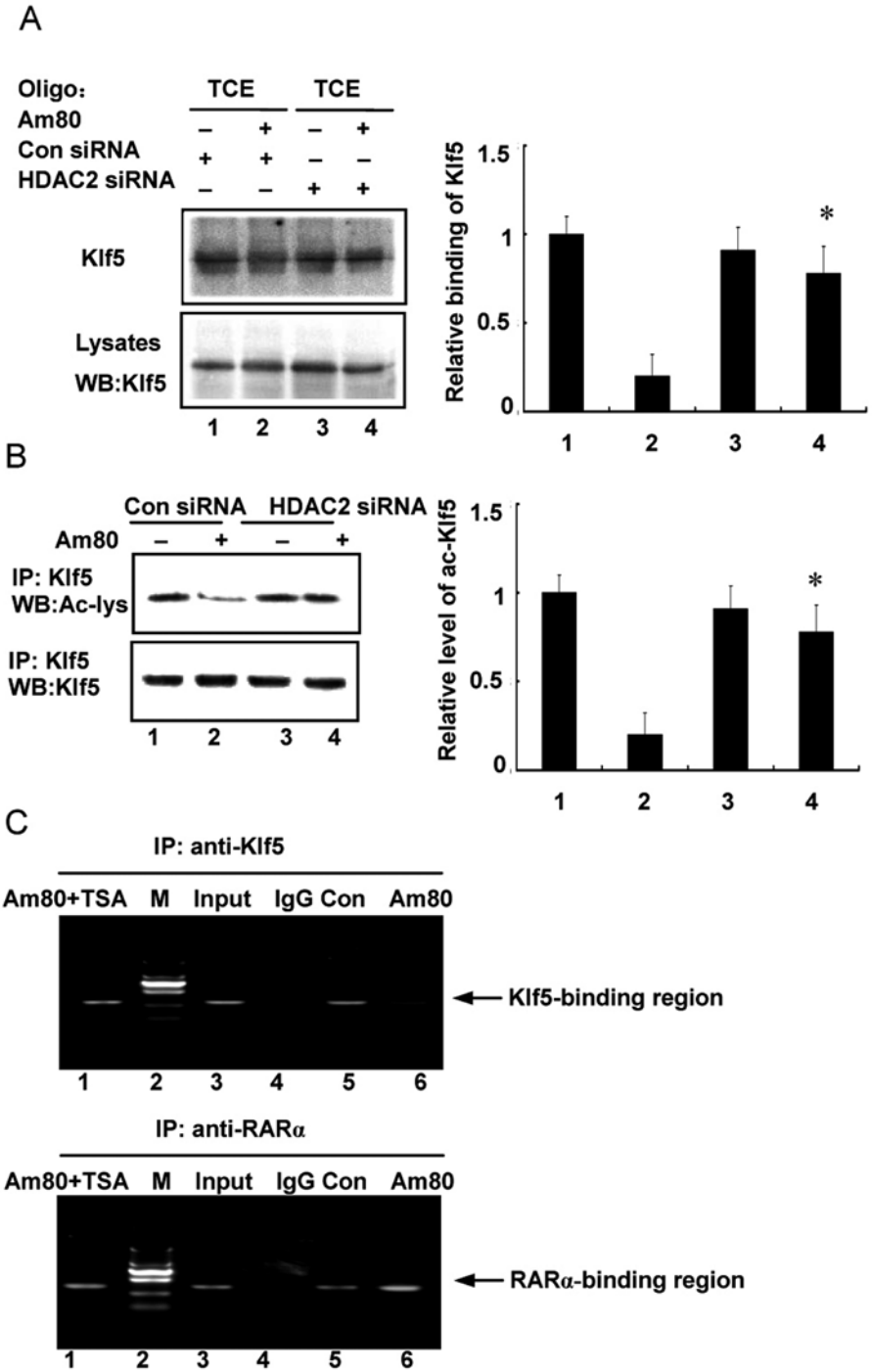

Figure 5 HDAC2 meditates the dissociation of Klf5 from the *p21* promoter. **(A)** VSMCs were cotransfected with control siRNA or with HDAC2 siRNA and treated with or without 2 μM Am80 for 2 h. The lysates were subjected to oligo pull-down assay using biotinylated double-strand oligonucleotides for Klf5-binding sites. Left, blots from a representative experiment are shown. Right, densitometry analysis was carried out and normalized to the input Klf5. The bars represent the means±S.E.M. of three independent experiments. **P* < 0.05. **(B)** VSMCs were cotransfected with control siRNA or with HDAC2 siRNA and treated with or without 2 μM Am80 for 2 h. Cell extracts were immunoprecipitated with antibody against Klf5 and immunoblotted with antibody against Ac-lys or Klf5. Left, blots from a representative experiment are shown. Right, densitometry analysis was carried out and normalized to the input Klf5. The bars represent the means±S.E.M. of three independent experiments. **P* < 0.05. **(C)** VSMCs were pretreated with TSA for 1 h before exposure to Am80 for 2 h. The binding of Klf5 and RARα to their respective elements was assessed by ChIP assay as described above.

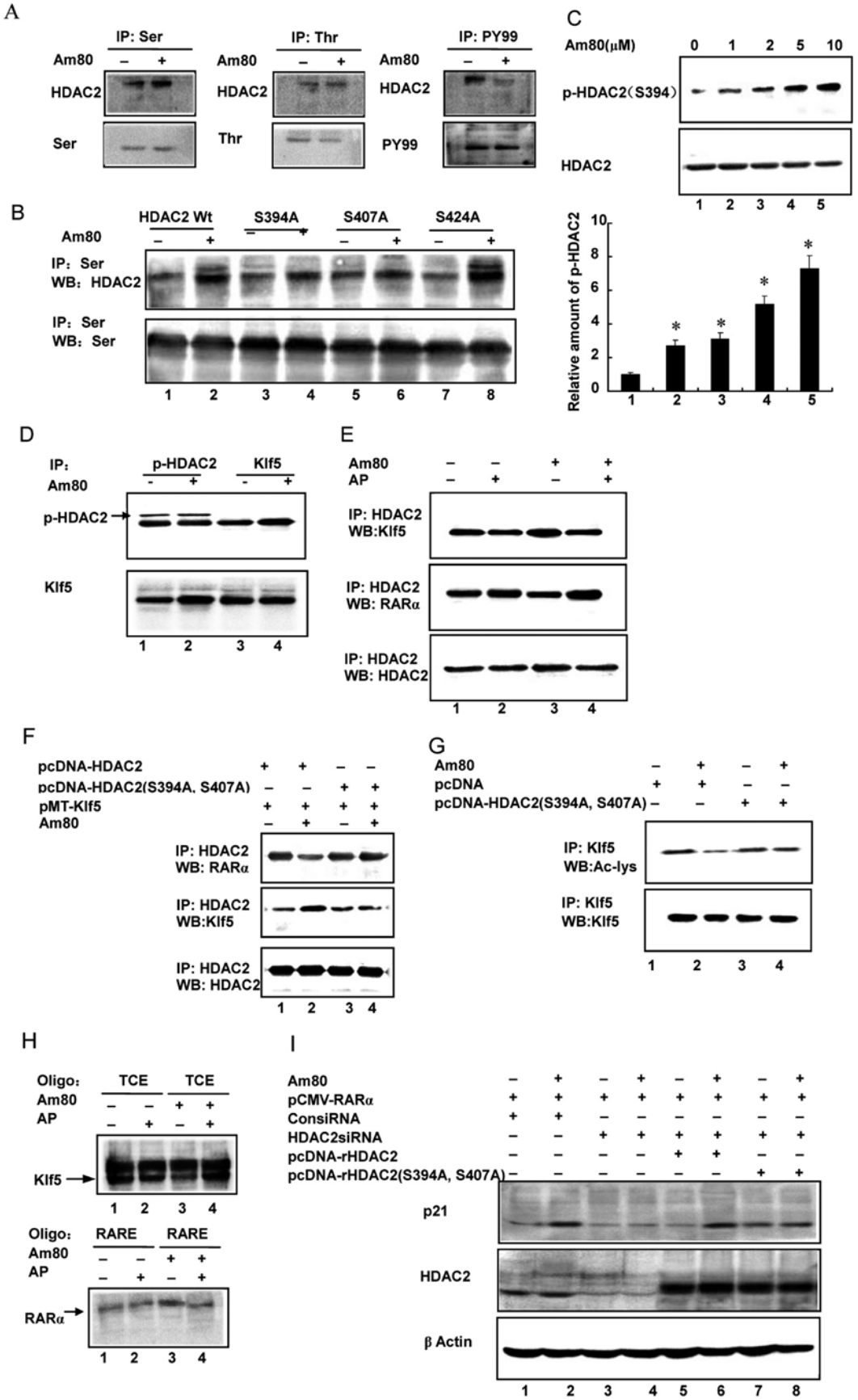
A
IP: Ser
IP: Thr
IP: PY99
Am80
HDAC2
Ser
Thr
PY99
B
HDAC2 Wt
S394A
S407A
S424A
IP: Ser
WB: HDAC2
WB: Ser
C
Am80(μM)
p-HDAC2(S394)
Relative amount of p-HDAC2
D
IP:
p-HDAC2
Klf5
E
AP
IP: HDAC2
WB:Klf5
WB: RARα
WB: HDAC2
F
pcDNA-HDAC2
pcDNA-HDAC2(S394A, S407A)
pMT-Klf5
G
pcDNA
IP: Klf5
WB:Ac-lys
H
Oligo:
TCE
RARE
RARα
I
pCMV-RARα
ConsiRNA
HDAC2siRNA
pcDNA-rHDAC2
pcDNA-rHDAC2(S394A, S407A)
p21
β Actin

induced Klf5 dissociation from its binding site (Figure 5A, compare lane 2 and lane 4). Silencing of HDAC2 expression also decreased Am80-induced deacetylation of Klf5 (Figure 5B). To further examine the importance of HDAC2 in the regulation of Klf5 binding to the *p21* promoter, we used TSA, an HDAC2 inhibitor, to block HDAC2 activity. ChIP assay showed that TSA treatment abrogated the inhibitory effect of Am80 on the binding of Klf5 to the *p21* promoter (Figure 5C, upper panel, compare lane 1 and lane 6), but had little effect on the binding activity of RARα (Figure 5C, lower panel, compare lane 1 and lane 6). Taken together, these data suggest that HDAC2 mediates Am80-induced deacetylation of Klf5 and its subsequent dissociation from the *p21* promoter.

HDAC2 phosphorylation induced by Am80 regulates Klf5 deacetylation and p21 expression

As Am80 increased Klf5 interaction with HDAC2 (e.g., see Figure 3E), we sought to determine the underlying mechanism by which Am80 induced their interaction. We first examined the effect of Am80 on HDAC2 phosphorylation. As shown in Figure 6A, Am80 markedly stimulated HDAC2 phosphorylation at serine residue(s) (left panel) rather than threonine residue(s) (middle panel). In contrast, HDAC2 phosphorylation on tyrosine residue(s) was significantly decreased following Am80 treatment (Figure 6A, right panel). HDAC2 contains three putative serine phosphorylation sites, S394, S407 and S424. To further determine which serine residue is phosphorylated in response to Am80, we mutated these three serine residues to alanine and carried out an *in vivo* phosphorylation assay. As shown in Figure 6B, only S424A mutant among the three mutants was phosphorylated in response to Am80 at levels comparable to those of wild-type HDAC2. In contrast, S407A and S394A mutants failed to be phosphorylated. These results strongly suggest that the major phosphorylation sites of HDAC2 are located at serine residues 394 and 407. To further corroborate this, an immunoblot analysis with phosphoserine 394-specific antiserum was performed and the results showed that Am80 markedly induced the phosphorylation of HDAC2 S394 in a dose-dependent manner (Figure 6C). We next investigated whether the phosphorylation of HDAC2 affected its interaction with Klf5 by Co-IP assay and found that, under Am80 treatment, there was an increased association between Klf5 and phosphorylated HDAC2 (Figure 6D). Moreover, incubation of HDAC2 immunoprecipitates with alkaline phosphatase decreased the interaction of HDAC2 with Klf5 induced by Am80 (Figure 6E, upper panel, compare lane 3 vs lane 4), suggesting that dephosphorylation of HDAC2 by phosphatase reduced its association with Klf5. To further identify the important role of HDAC2 phosphorylation in the phosphorylation-deacetylation switch of transcriptional repression complex, we transfected the expression vectors for Klf5, wild-type HDAC2 or its S394A/S407A mutant into 293A cells, and examined Klf5's interaction with HDAC2 and Klf5 acetylation level. As shown in Figure 6F, mutation of phosphorylation sites (S394A and S407A) of HDAC2 abrogated Am80-induced interaction of HDAC2 with

Figure 6 Am80 induces HDAC2 phosphorylation and Klf5 deacetylation. **(A)** VSMCs were treated with or without 2 μM Am80 for 2 h. Cell lysates were immunoprecipitated by antibody against phosphoserine (p-Ser, left panel), phosphothreonine (p-Thr, middle panel) or phosphotyrosine (p-PY99, right panel), followed by immunoblotting using anti-HDAC2 antibody. **(B)** 293A cells were transfected with expression vectors for wild-type HDAC2 (HDAC2 WT) and its mutants of phosphorylation sites (serines 394, 407 and 424) and treated with or without Am80 (2 μM). Cell lysates were immunoprecipitated with antibody against phosphoserine and immunoblotted with antibody against HDAC2. **(C)** VSMCs were treated with indicated concentrations of Am80 for 2 h. Cell lysates were immunoblotted with the phospho-HDAC2-specific antibody (S394). Upper, blots from a representative experiment are shown. Lower, densitometry analysis. The bars represent the means±S.E.M. of three independent experiments. **P* < 0.05. **(D)** VSMCs were treated with or without Am80 (2 μM) for 2 h. Cell lysates were immunoprecipitated with anti-phospho-HDAC2-specific antibody (S394) or anti-Klf5 antibody. The immunoprecipitates were immunoblotted with antibody against Klf5 or phospho-HDAC2 (S394). **(E)** VSMCs were treated with or without Am80 (2 μM) for 2 h; cell lysates were immunoprecipitated with anti-HDAC2 antibody. The immunoprecipitates were incubated with (+AP) or without (−AP) alkaline phosphatase, and were detected by anti-Klf5 or anti-HDAC2 antibodies. **(F)** 293A cells were transfected with expression vectors for Klf5, HDAC2 or its mutant of phosphorylation sites (S394A and S407A) and treated with or without Am80 (2 μM) for 2 h. Cell lysate was immunoprecipitated with anti-HDAC2 antibody and immunoblotted with antibody against Klf5 or HDAC2. **(G)** 293A cells were transfected with expression plasmid for HDAC2 phosphorylation site mutant (S394A, S407A) and treated with or without Am80 (2 μM) for 2 h. Cell lysate was immunoprecipitated with anti-Klf5 antibody and immunoblotted with antibody against Ac-lys or Klf5. **(H)** VSMCs were treated with or without Am80 (2 μM) for 2 h. Cell lysates were incubated with or without alkaline phosphatase and pulled down using biotinylated double-strand oligonucleotides for Klf5-binding sites (upper panel) or RARα-binding sites (lower panel). DNA-bound proteins were analyzed by western blot for Klf5 or RARα. **(I)** For rescue experiment, A293 were transfected first with HDAC2 siRNA for 24 h, then pcDNA-rHDAC2, or its mutant of phosphorylation sites (S394A and S407A) was transfected again for another 24 h, and cells were treated with or without Am80 (2 μM). p21 expression was analyzed by western blot assay.

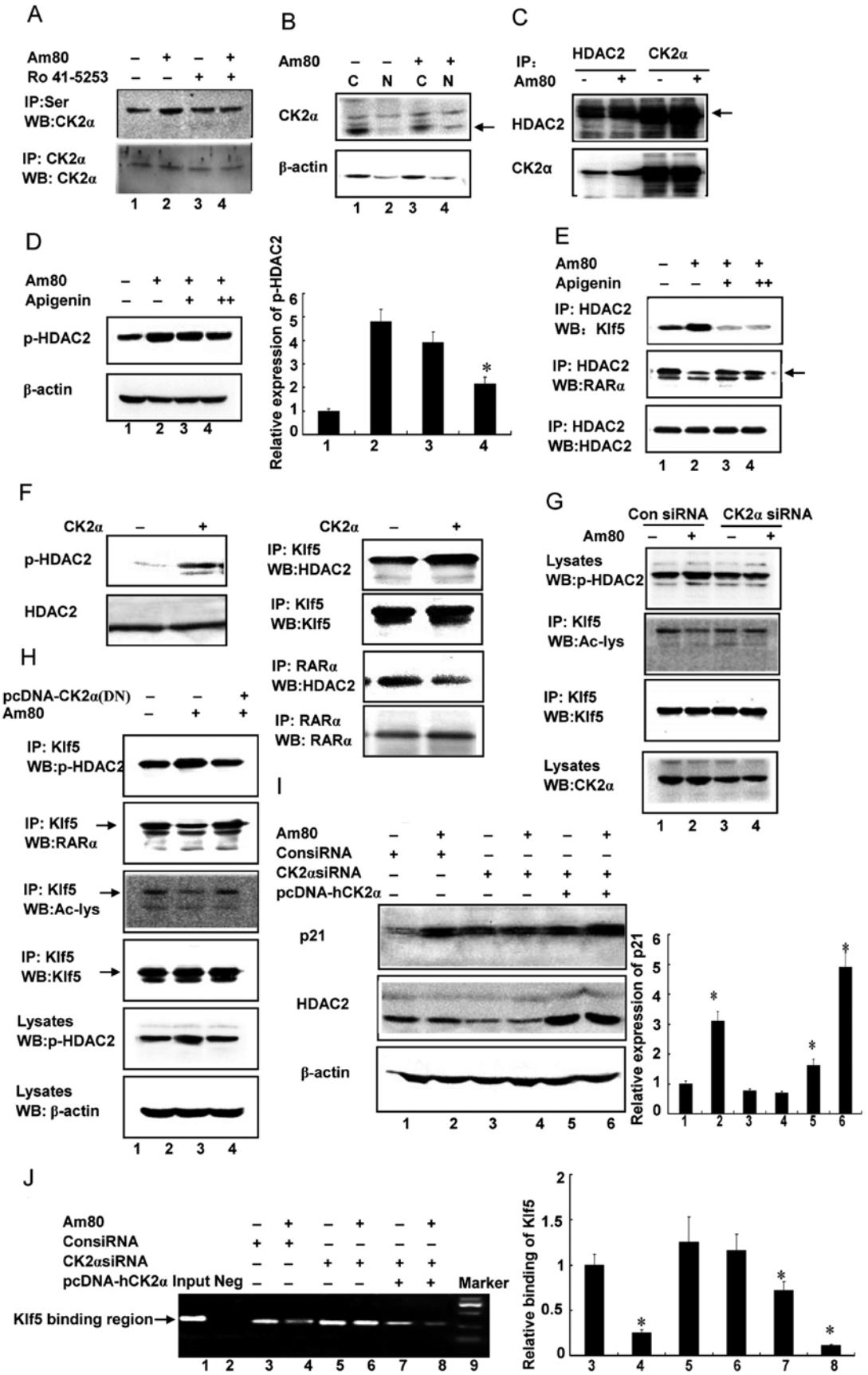
A
Am80 – + – +
Ro 41-5253 – – + +
IP:Ser
WB:CK2α
IP: CK2α
WB: CK2α
1 2 3 4
B
Am80 – – + +
C N C N
CK2α
β-actin
1 2 3 4
C
IP: HDAC2 CK2α
Am80 - + - +
HDAC2
CK2α
D
Am80 – + + +
Apigenin – – + ++
p-HDAC2
β-actin
1 2 3 4
Relative expression of p-HDAC2
E
Am80 – + + +
Apigenin – – + ++
IP: HDAC2
WB: Klf5
IP: HDAC2
WB:RARα
IP: HDAC2
WB:HDAC2
1 2 3 4
F
CK2α – +
p-HDAC2
HDAC2
CK2α – +
IP: Klf5
WB:HDAC2
IP: Klf5
WB:Klf5
IP: RARα
WB:HDAC2
IP: RARα
WB: RARα
G
Con siRNA CK2α siRNA
Am80 – + – +
Lysates
WB:p-HDAC2
IP: Klf5
WB:Ac-lys
IP: Klf5
WB:Klf5
Lysates
WB:CK2α
1 2 3 4
H
pcDNA-CK2α(DN) – – +
Am80 – + +
IP: Klf5
WB:p-HDAC2
IP: Klf5
WB:RARα
IP: Klf5
WB:Ac-lys
IP: Klf5
WB:Klf5
Lysates
WB:p-HDAC2
Lysates
WB: β-actin
1 2 3 4
I
Am80 – + – + – +
ConsiRNA + + – – – –
CK2αsiRNA – – + + + +
pcDNA-hCK2α – – – – + +
p21
HDAC2
β-actin
1 2 3 4 5 6
Relative expression of p21
J
Am80 – + – + – +
ConsiRNA + + – – – –
CK2αsiRNA – – + + + +
pcDNA-hCK2α Input Neg – – – – + +
Marker
Klf5 binding region
1 2 3 4 5 6 7 8 9
Relative binding of Klf5
3 4 5 6 7 8

Klf5. Figure 6G showed that the mutation of phosphorylation sites of HDAC2 also abolished Am80-induced deacetylation of Klf5, suggesting that deacetylation of Klf5 requires the phosphorylation of HDAC2. Given that deacetylation of Klf5 facilitates its dissociation from the *p21* promoter (see earlier sections), one would predict that an effect of HDAC2 phosphorylation is to reduce Klf5 binding to the *p21* promoter, by positively regulating Klf5 deacetylation, and thus increase p21 expression. Indeed, Figure 6H shows that treating the cell lysates with alkaline phosphatase to remove HDAC2 phosphorylation resulted in a marked increase in Klf5 binding to the oligo containing Klf5-binding site (Figure 6H, upper panel, lane 4), but had little effect on RARα binding to its sites (Figure 6H, lower panel). To further dissect the role of endogenous HDAC2 and its phosphorylation in Am80-induced p21 expression, we knocked down the expression of endogenous HDAC2 and then transfected the RNAi-resistant S394A/S407A mutant of HDAC2 or wtHDAC2 into VSMCs, respectively, and examined the expression of p21. As shown in Figure 6I, Am80 efficiently induced p21 expression in control siRNA-treated cells, and the induction was blunted by the knockdown of endogenous HDAC2, consistent with an interesting role of endogenous HDAC2 in mediating both the repression of *p21* under basal conditions (see Figure 6I and Figure 2C) and the efficient activation of *p21* under Am80 treatment (Figure 6I). Importantly, Am80 induction of p21 expression was restored by re-expression of the RNAi-resistant wtHDAC2 but not the S394A/S407A mutant, suggesting that HDAC2 phosphorylation at S394 and S407 plays a critical role in mediating efficient induction of p21 expression by Am80 (Figure 6I).

Am80 induces HDAC2 phosphorylation through a CK2α-dependent pathway

We inspected the amino acid sequence of HDAC2 by computer analysis and found that there is a typical CK2α target site. In addition, previous studies have shown that HDAC2 could be phosphorylated by CK2α [35, 36]. We next sought to determine whether CK2α was involved in Am80-induced phosphorylation of HDAC2. First, we detected whether Am80 could activate CK2α. As shown in Figure 7A, phosphorylation of CK2α was significantly increased by Am80 treatment. Ro 41-5253, a RARα-specific antagonist, completely blocked Am80-induced phosphorylation of CK2α. Since HDAC2 is primarily located in the nucleus of VSMCs, we examined whether Am80 could affect the subcellular localization of CK2α and its interaction with HDAC2. As shown in Figure 7B, under basal conditions without Am80 stimulation, CK2α was mainly localized in the cytoplasm. After Am80 stimulation for 1 h, CK2α was partly shuttled to the nucleus from cytoplasm. We also analyzed anti-HDAC2 immunoprecipitates by immunoblotting with anti-CK2α antibody and found that HDAC2 bound to CK2α under

Figure 7 Am80 induces HDAC2 phosphorylation through a CK2α-dependent pathway. **(A)** VSMCs were pretreated with or without Ro 41-5253 for 1 h, followed by exposure to Am80 (2 μM) for 2 h. The phosphorylation of CK2α was detected by immunoprecipitating with anti-phosphoserine antibody and immunoblotting with anti-CK2α antibody. **(B)** VSMCs were treated with Am80 for 2 h and cytoplasmic and nuclear extracts were prepared. In order to evaluate the ratio of CK2α localized in the cytoplasm (C) and nucleus (N) accurately, a 10% volume of each extract was subjected to immunoblotting with anti-CK2α antibody. The right panel shows the relative expression levels of CK2α in each compartment. **(C)** VSMCs were lysed in IP buffer containing protease and phosphatase inhibitors. Cell lysates were immunoprecipitated with anti-CK2α antibodies or preimmune serum as negative control. The immunoprecipitates were immunochemically stained with anti-HDAC2 and anti-CK2α antibodies. **(D)** VSMCs were treated with or without Apigenin, or Am80 (2 μM) for 2 h. The phospho-HDAC2 was determined as described above. Left, blots from a representative experiment are shown. Right, densitometry analysis. The bars represent the means ± S.E.M. of three independent experiments. **P* < 0.05. **(E)** VSMCs were treated with or without Apigenin, or Am80 (2 μM) for 2 h. The HDAC2 interaction with Klf5 or RARα was determined using Co-IP as described above. **(F)** The GST-Klf5, GST-HDAC2 and GST-RARα fusion proteins were incubated with the active CK2α and ATP for 15 min at 37 °C, and then aliquots of the mixtures were immunoblotted with phospho-HDAC2 antibody (left panel); other aliquots were immunoprecipitated by anti-Klf5 or anti-RARα antibodies and immunoblotted with anti-HDAC2, anti-Klf5 and anti-RARα antibodies, respectively (right panel). **(G)** VSMCs were transfected with CK2α siRNA or control siRNA for 24 h and treated with or without Am80 (2 μM). The phospho-HDAC2 and acetylated-Klf5 were detected by western blotting and Co-IP as described above. Klf5 and CK2α were also analyzed by immunoblotting with their respective antibody. **(H)** VSMCs were transfected with dominant-negative CK2α-expressing plasmids and treated with or without Am80 (2 μM). The phospho-HDAC2, acetylated Klf5, the phospho-HDAC2 interaction with Klf5, and Klf5 interaction with and RARα were determined as described above. **(I)** VSMCs were transfected first with CK2α siRNA for 24 h, then pcDNA-hCK2α, or CK2α (DN) was transfected again, respectively, for another 24 h, and cells were treated with or without Am80 (2 μM). p21 expression was detected by western blot assay. **P* < 0.05. **(J)** VSMCs were transfected first with CK2α siRNA for 24 h, then pcDNA-hCK2α was transfected again for another 24 h, and cells were treated with or without Am80 (2 μM). The binding of Klf5 to the TCE element was detected by ChIP assay. **P* < 0.05.

basal conditions and that Am80 promoted the interaction of CK2α with HDAC2 in the nucleus (Figure 7C). Then, we further examined whether CK2α mediated Am80-induced phosphorylation of HDAC2. The results showed that apigenin, a CK2α inhibitor, significantly decreased the phosphorylation of HDAC2 induced by Am80 in a dose-dependent manner (Figure 7D), blocked Am80-induced interaction between Klf5 and HDAC2 (Figure 7E, upper panel), and reversed the inhibitory effect of Am80 on the interaction of RARα with HDAC2 (Figure 7E, middle panel). To further address the functional role of CK2α in HDAC2 phosphorylation and HDAC2's interaction with Klf5 or RARα, we performed an *in vitro* phosphorylation assay. GST-tagged HDAC2, RARα and Klf5 were expressed in *Escherichia coli* cells, and purified by Glutathione Sepharose 4B-coupled beads and incubated with CK2α. The reaction products were subjected to immunoblotting with anti-phospho-Ser^{394} HDAC2 antibody. Figure 7F showed that Ser^{394} of HDAC2 could be phosphorylated by CK2α (left panel). The interaction between Klf5 and HDAC2 increased after HDAC2 phosphorylation by CK2α (Figure 7F, right panel). By contrast, the phosphorylation of HDAC2 by CK2α decreased its association with RARα (Figure 7F, right panel). These results indicate that HDAC2 associates mainly with RARα in the unphosphorylated form under basal conditions without Am80 stimulation, but interacts with Klf5 when it is phosphorylated by CK2α. We also evaluated the effect of a dominant-negative CK2α or CK2α siRNA on the phosphorylation of HDAC2. As shown in Figure 7G, knockdown of CK2α by siRNA prevented both HDAC2 phosphorylation (first panel, compare lane 2 and lane 4) and Klf5 deacetylation (second panel, compare lane 2 and lane 4) induced by Am80.

Furthermore, we transfected a dominant-negative form of CK2α (CK2α DN) into VSMCs and found that forced expression of the dominant-negative CK2α decreased HDAC2 phosphorylation and Klf5 deacetylation and increased the interaction between RARα and Klf5 in the presence of Am80 (Figure 7H, compare lane 2 and lane 3). These results suggest that the activity of CK2α is required for the phosphorylation of HDAC2 induced by Am80. On the basis of these findings, HDAC2 phosphorylation-dependent deacetylation of Klf5 triggered by CK2α seems to switch the transcription-regulatory programs of *p21*. To further test this, we knocked down the expression of endogenous CK2α and then transfected the RNAi-resistant wtCK2α into VSMCs, and examined the expression of p21. Western blot analysis showed that knockdown of CK2α abolished the induction of p21 expression by Am80 (Figure 7I, compare lane 2 and lane 4). However, re-expression of CK2α could restore Am80-induced p21 expression (Figure 7I). We also examined Klf5 binding to the *p21* promoter by ChIP assay. As expected, Am80 treatment decreased Klf5 binding to the *p21* promoter, but this Am80-induced reduction of Klf5 binding was abolished in CK2α knockdown cells (Figure 7J, compare lane 4 and lane 6). When CK2α was re-expressed, cells recovered the ability to downregulate Klf5 binding to the *p21* promoter in the presence of Am80 (Figure 7J, compare lane 6 and lane 8). Taken together, these findings strongly suggest that Am80 induces HDAC2 phosphorylation at Ser^{394} and Ser^{407} via a CK2α-dependent pathway and that phosphorylation of HDAC2 in turn regulates its interaction with Klf5 and/or RARα, resulting in Klf5 deacetylation and dissociation from the *p21* promoter as well as consequent activation of p21 expression.

Upregulation of p21 expression accompanies Am80-mediated inhibition of neointima formation

To address the direct effects of Am80 on vascular remodeling, we tested the effect of orally administered Am80 on neointima formation in the rat models of balloon-induced vascular injury. Figure 8A showed that neointima formation was markedly increased at 2 weeks after balloon injury, and that orally administered Am80 significantly reduced neointima formation, which was accompanied by upregulation of p21 expression and inhibition of VSMC proliferation, as assessed by immunohistochemical staining using anti-p21 and anti-PCNA antibodies. As proliferation is coupled with cell cycle progression, we next examined the effect of Am80 on cell cycle progression using cultured VSMCs. As shown in Figure 8B, Am80 induced G0/G1 cell cycle arrest, increasing the G0/G1 population by 16% over non-treated cells and decreasing S-phase cells by about 37% at 24 h after Am80 treatment. MTT assay also showed that Am80 significantly inhibited the proliferation of cultured VSMCs (Figure 8C). These data support that Am80 inhibits proliferation by inducing the expression of p21. We further analyzed whether vascular intimal injury and Am80 treatment could affect HDAC2 phosphorylation in the intact animal. As shown in Figure 8D, HDAC2 existed as a hypophosphorylated form in the uninjured vessel wall, and the endothelial injury modestly induced HDAC2 phosphorylation within 3 h. Orally administered Am80 further increased the injury-induced phosphorylation of HDAC2 (Figure 8D). We next examined the link between HDAC2 phosphorylation and its interaction with Klf5 or RARα by Co-IP assay, and found that the interaction between HDAC2 and Klf5 increased after Am80 treatment, while the interaction between HDAC2 and RARα significantly decreased following HDAC2

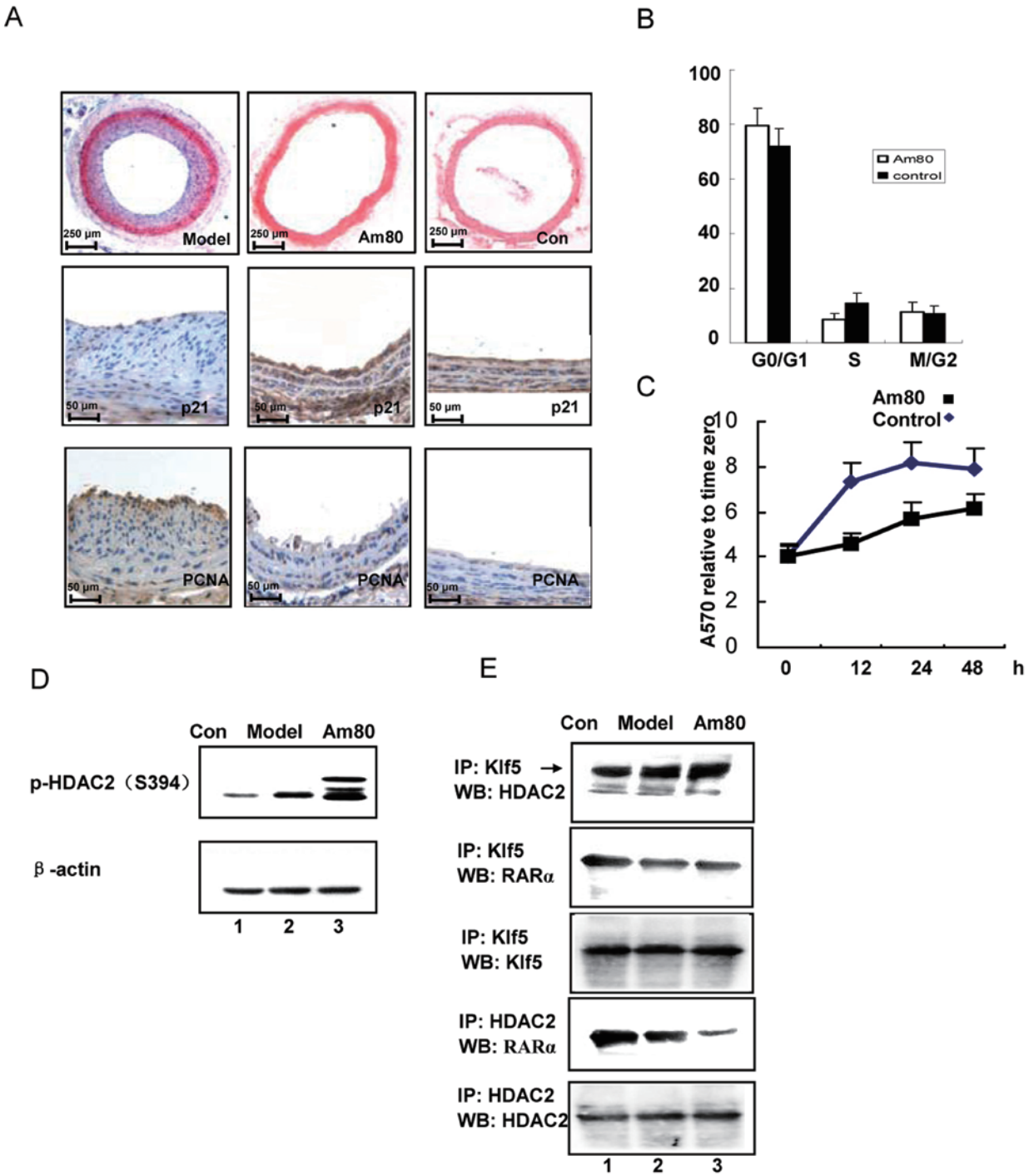

Figure 8 Am80 reduces neointima formation by upregulating p21 expression. **(A)** Neointima hyperplasia 14 days after balloon injury. Representative sections of hematoxylin-eosin-stained arterial sections from control, model, or Am80-treated animals. VSMC proliferation index was evaluated by immunohistochemical staining using anti-PCNA and anti-p21 antibodies. Am80 was given to rats by mouth for 24 h, followed by balloon injury as described in Materials and Methods. **(B)** Effect of Am80 on VSMC proliferation as assessed by flow cytometry. VSMCs were stained with propidium iodide to evaluate DNA content by flow cytometry. **(C)** Effect of Am80 on VSMC proliferation as assessed by MTT assay. Experiments were performed in triplicate, and each value is the mean ± S.E.M. of three independent experiments. **P* < 0.05. **(D)** 3 h after balloon injury, the arteries were harvested, and western blot analysis was performed with antibody against phospho-HDAC2. **(E)** Interactions between HDAC2, RARα and Klf5 were assessed by Co-IP assay as described above.

phosphorylation induced by Am80 (Figure 8E), consistent with the results obtained with the cultured cells. These findings provide *in vivo* evidence supporting the new molecular mechanism revealed by our study in cultured cells.

Discussion

The transcriptional regulation of *p21*, which is a member of the Cip/Kip family of CKIs, is tightly involved in growth inhibition of VSMCs [23]. Here, we report that Klf5, RARα and HDAC2 form a repression complex to synergistically inhibit the expression of p21 under basal conditions. Upon agonist stimulation of RARα, Klf5 was deacetylated and dissociated from its binding sites on the *p21* promoter, thus relieving its repressive effect on p21 expression. Thus, deacetylation of Klf5 seems to be a molecular switch affecting the function of Klf5 and the transcriptional regulatory programs governing cell proliferation. In addition, Suzuki *et al*. identified that Klf5 plays a central role in cardiovascular pathologies by regulating the expression of cyclin D1 and cyclin-dependent kinase and specific stimulation of cell growth [3]. That is to say, Klf5, on the one hand, inhibits the expression of p21, and, on the other hand, stimulates the expression of Cyclin D and promotes cell proliferation. It has been known that Klf5's activities are regulated by its interaction with cofactors, acetylation by the acetylase p300 and phosphorylation by p38 and Smad signaling [25, 34, 37, 38]. Given our understanding of the actions and regulation of this family of transcription factors and their cofactors, they may serve as an excellent target for further investigations on the role of DNA-binding transcription factors in transcription at the chromatin level, especially with regard to their functional interaction with histone chaperones.

In the present study, we found that functional interaction of RARα with Klf5 resulted in the synergistic suppression of p21 expression under basal conditions (Figure 1). This finding is noteworthy because, to our knowledge, many of the genes identified to date as direct targets of Klf5 are transactivated by Klf5. So we speculate that the inhibitory effect of Klf5 on *p21* might involve its interaction with other co-repressors; the latter, we identified, are RARα and HDAC2 (Figure 2). Histone acetylation/deacetylation is a fundamental mechanism for the control of gene expression. Histone acetyltransferases activate transcription through acetylation of histones, and HDACs antagonize this activity and repress transcription [39]. Individual HDAC enzymes may have a distinct biological function and may be regulated independently [40, 41]. HDACs comprise at least 17 members, of which class I HDACs (HDACs 1-3, 8 and 11) are widely expressed and are found in most cell types, and appear to be dedicated to the control of cell proliferation and survival, whereas class II HDACs (HDACs 4, 5, 7 and 9) may be involved in cellular differentiation [42]. It is clear that not all class I HDACs function in the same way, as they are often components of distinct corepressor complexes. For example, HDAC1 and HDAC2 interact with Snail and Sin3A to form a corepressor complex to repress E-cadherin expression [43]; HDAC3 is associated with corepressors N-coR and SMRT mediating transcriptional repression by the thyroid hormone receptor (TR) [44]; krüppel-like factor 4 (Klf4) has been found to physically associate with HDAC2 and recruit this protein to SMC gene promoters and regulate their expression [45, 46]. Our experiments revealed that HDAC2 is recruited to the RARE site by RARα, and Klf5 participates in this repressive complex by interacting with RARα directly (Figures 1 and 2). Taken together, we propose a model for the regulation of p21 expression through recruitment of HDAC2 and Klf5 by unliganded RARα to the *p21* promoter, which in turn represses *p21* transcription.

Upon Am80 treatment, liganded RARα recruits p300 and promotes local acetylation [47], and the repressive complex formed by Klf5, RARα and HDAC2 is disrupted, leading to activation of the *p21* promoter. On the one hand, ligand binding of RARα promoted the dissociation of Klf5 and RARα (Supplementary information, Figure S3A), and switched the binding partner of RARα from HDAC2 (Supplementary information, Figure S3B) to p300, resulting in RARα acetylation (Supplementary information, Figure S3C and S3D), and the increase of RAR binding activity to the *p21* promoter (Supplementary information, Figure S3E), increasing p21 expression (Supplementary information, Figure S3F). On the other hand, HDAC2, which dissociated from liganded RARα, underwent Am80-induced phosphorylation and interacted with Klf5, resulting in deacetylation of Klf5 and the release of Klf5 from the repressive complex and de-repression of the *p21* promoter. Our results indicate that HDAC2 shifting from RARα to Klf5 plays a key role in the regulation of p21 expression. Recently, Lin *et al.* reported that statins induced p21 expression through the dissociation of HDAC1/2 and association of CBP, leading to histone acetylation on the Sp1 sites of the *p21* promoter [48]. Delarue *et al*. found that antitumor agents farneyltransferase inhibitors and geranylgeranyltransferase I inhibitors upregulate Rho expression through the dissociation of HDAC and association of p300, leading to histone acetylation on the RhoB promoter [49]. The incapability of HDACs to bind DNA directly indicates that HDACs are recruited indirectly to the promoter through

association with other transcription factors. Although previous reports also demonstrated that SAHA releases HDAC from Sp1 sites on the *p21* promoter [48, 50], we are the first to show that Am80 compels the dissociation of HDAC2 from RARE sites and enhances the binding of RARα to the *p21* promoter. These findings demonstrate that molecules within transcriptional regulatory complexes are dynamically exchanged during transcriptional activation, which may involve protein modifications. Although the precise molecular events need to be clarified in future studies, our results clearly indicate that Am80 induces ordered and sequential protein modifications and exchanges, including deacetylation and exchange of co-regulators.

Our results support a model in which HDAC2 is required for the proper formation of transcriptional regulatory complexes. It has been shown that Am80-induced growth arrest is dependent on the activation of some signaling cascades, including p38, JNK and ERK in VSMCs [51]. While we do not yet know the precise signaling events leading to the modification of Klf5 and RARα in response to Am80, the phosphorylation of HDAC2 is likely a key step in triggering this process. We show that Am80 activates CK2α, which then phosphorylates HDAC2. Phosphorylation of HDAC2 increases its interaction with Klf5, which in turn triggers Klf5 deacetylation and its subsequent dissociation from the promoter of *p21*. We showed that Am80 elicits phosphorylation of HDAC2 at S394 and S407 in a CK2α-dependent manner. Importantly, we found that phosphorylation of HDAC2 at these sites is a prerequisite for its interaction with Klf5 and the Klf5 deacetylation that subsequently triggers the dissociation of Klf5 from the promoter of *p21*. In agreement with our data, similar regulatory events were previously described for p53 and NF-κB, which were phosphorylated and acetylated in response to tumor necrosis factor α [52].

Because a growing body of evidence indicates that RARs are a key class of transcription factors governing cell proliferation, RAR agonists are now considered to be an attractive agent for the development of therapeutic strategies against pathophysiological vascular remodeling [29, 31]. However, their therapeutic use has been precluded by serious adverse effects such as skin or liver toxicity and teratogenesis because RARs are widely expressed in various tissues [53]. To further uncover the possible other mechanism for Am80-induced growth inhibition, gene profiling experiment was performed after treatment with or without Am80. The results of cDNA microarray showed that Am80 could induce or inhibit the expression of distinct genes. We found that Am80 could indeed induce the expression of growth-inhibiting genes, such as p21 and p53, and inhibited the pro-proliferation genes, such as Cdk2, VEGFA, FGF2 and so on (Supplementary information, Table S1). These results indicate that Am80 regulates SMC growth by causing the genome-wide response (Supplementary information, Figure S4). Therefore, strategies focusing on RARα also need to be evaluated carefully for possible side effects. Unlike RARα, Klf5 expression shows a cell-specific pattern; further elucidation of the transcriptional regulatory programs involving RARα and Klf5 may hold potential for the development of more selective modulators of p21 expression.

In summary, the results of our present study provide novel evidence showing that Klf5, RARα and HDAC2 form a transcriptional repression complex on the *p21* promoter and synergistically inhibit p21 expression in resting cells (Figure 9). Upon RARα activation by Am80, ligand-activated RARα dissociates from HDAC2 and interacts with p300 and is acetylated, subsequently leading to the increase in the ability of RARα to activate the *p21* promoter. In addition, HDAC2 phosphorylation induced by Am80 promotes its interaction with Klf5, leading to Klf5 deacetylation. Deacetylated Klf5 dissociates from the *p21* promoter, resulting in the disruption of the transcriptional repression complex formed by Klf5, RARα and HDAC2, allowing for the optimum activation of the transcription of *p21* (Figure 9). Our study uncovers a novel phosphorylation-deacetylation cascade mediating RAR agonist-induced p21 expression, and a similar scheme may also operate in the regulation of expression of other genes.

Materials and Methods

Cell culture and treatment

Male Sprague-Dawley rats were anesthetized with sodium pentobarbital (Sigma); the aorta was removed, and VSMCs were isolated and cultured as previously described [54]. VSMCs and 293A cells were maintained and passaged in Dulbecco's modified Eagle's medium (DMEM) with 10% fetal bovine serum (HyClone), 100 U/ml of penicillin and 100 μg/ml of streptomycin. The experiments were initiated when the cells reached 70% confluence, unless stated otherwise. For studies on the effects of Am80, the cells were starved for 24 h and then left untreated or treated for 2 h with the indicated concentration of Am80 [25].

Adenovirus expression vector and plasmids

The full-length rat Klf5 cDNA was cloned into the pAd/CMV/V5-DEST vector (Invitrogen) to create the Klf5 adenovirus pAd-Klf5. The resulting constructs were packaged in 293A cells (ATCC) by transfection with Lipofectamine 2000 (Invitrogen) according to the manufacturer's instructions. pCMV-hRARα (kindly provided by Dr Ronald M Evans, Howard Hughes Medical Institute, The Salk Institute, San Diego, CA, USA) [55], pMT3-Klf5 (kindly provided by Dr Nandan Mandayam, Emory University School

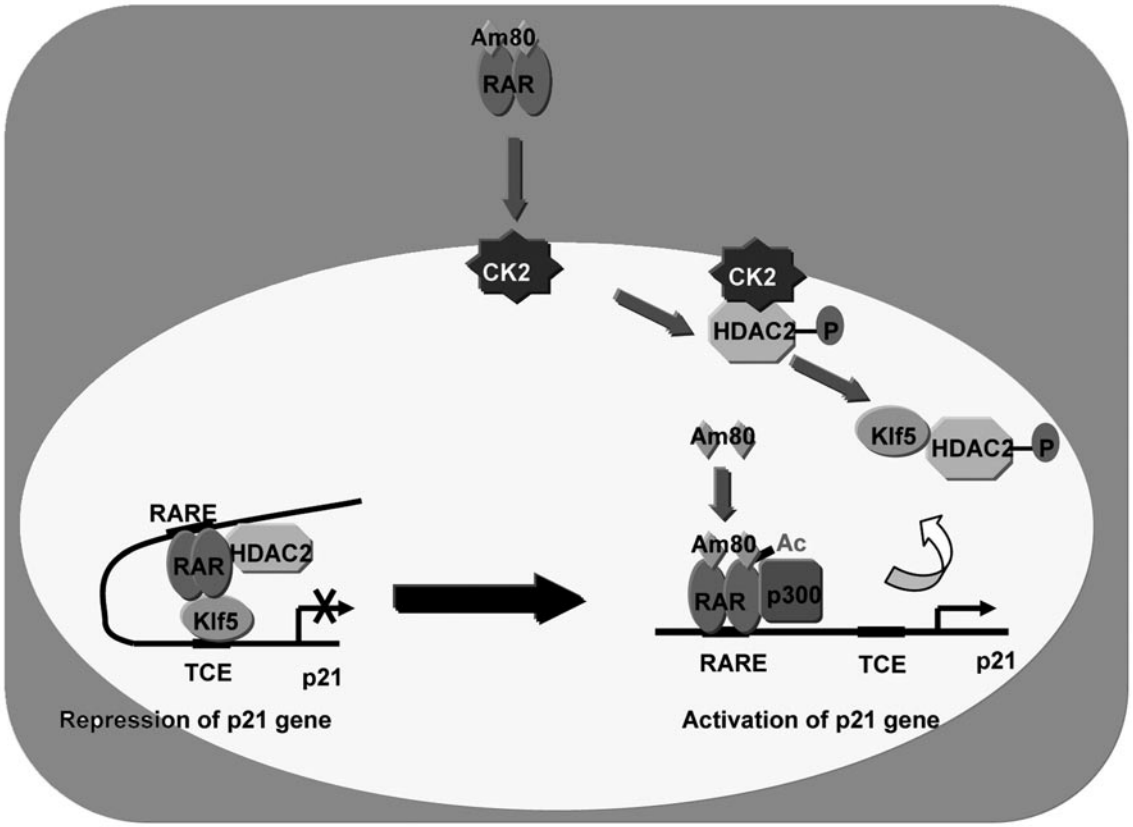

Figure 9 Model illustrating the mechanism by which Am80 induces p21 expression. In quiescent cells, p21 expression is repressed by HDAC2, RARα and Klf5 repressive complex occupancy of the *p21* promoter. Liganded RARα activates the transcription of *p21* directly. In response to Am80, CK2α is translocated into the nucleus and recruited to the *p21* promoter, leading to the phosphorylation of HDAC2 at S394 and S407. The phospho-HDAC2 interacts with Klf5 and is required for the subsequent deacetylation of Klf5. Deacetylated Klf5 dissociates from the *p21* promoter, resulting in the alleviation of the *p21* repression.

of Medicine) [56], pcDNA-HDAC2 (kindly provided by Dr Kim Young-eui, Sungkyunkwan University School of Medicine) [57], Flag-p300 (kindly provided by WR Harrison, BCM Baylor College of Medicine) and pcDNA-HA-E1A12S (kindly provided by Dr Mahvash Tavassoli, King's College London) [58] was transfected to VSMCs with ESCORT-IV (Sigma), according to the manufacturer's instructions. RARα, Klf5 and HDAC2 siRNAs were designed by custom Accell SMARTpool (Dharmacon). The Accell siRNA delivery medium (Dharmacon) was used according to the manufacturer's recommendations.

For rescue experiments, A293 or rVSMCs were transfected first with HDAC2 or CK2α siRNA for 24 h; then pcDNA-rHDAC2, its mutant of phosphorylation sites (S394A and S407A) or pcDNA-hCK2α, respectively, was transfected again for another 24 h, and cells were treated with or without Am80 (2 μM). p21 expression was detected by western blot assay.

Reporter gene assay

293A cells were transfected with a luciferase-harboring *p21* promoter (gift from Dr Bert Vogelstein, The Johns Hopkins Medical Institutions) [59], pMT-Klf5, pcDNA-HDAC2, pCMV-RARα and Flag-p300 using Lipofectamine 2000 (Invitrogen) according to the manufacturer's protocol. The cells were harvested after 48 h, and the activities of both firefly luciferase and Renilla luciferase were measured in the LB 955 Luminometer system using the dual luciferase reporter system (Promega) according to the manufacturer's recommendations [60]. The activity of firefly luciferase was normalized to that of Renilla luciferase. A minimum of three independent transfections was performed for each experimental group.

Western blot analysis

The cells were lysed with 150 mM NaCl, 50 mM Tris-HCl (pH 7.5), 1% Nonidet P-40, 0.5% sodium deoxycholic acid and complete protease inhibitor mixture tablets (Roche Applied Science), and the protein was then isolated. Total protein (70 μg) from each sample was separated by 8% or 12% SDS-PAGE and transferred onto a polyvinylidene fluoride membrane (Millipore). The membranes were blocked with 5% milk in TTBS for 2 h at room temperature and incubated overnight at 4 °C using the following primary antibodies: 1:500 rabbit anti-Klf5 (Santa Cruz Biotechnology), 1:500 rabbit anti-RARα (Santa Cruz Biotechnology), 1:500 rabbit anti-HDAC2 (Santa Cruz Biotechnology), 1:1 000 rabbit

antiphospho-HDAC2 (Cell Signaling), 1:1 000 rabbit antiphospho-Ser (Sigma), 1:500 rabbit antiphospho-Thr (Santa Cruz Biotechnology), 1:500 antiphospho-PY99 (Santa Cruz Biotechnology), 1:500 anti-Ac-lys (Santa Cruz Biotechnology), 1:200 anti-p21 (Santa Cruz Biotechnology), 1:500 antiphospho-PY99 (Santa Cruz Biotechnology) and 1:1 000 mouse anti-β-actin (Santa Cruz Biotechnology). The membranes were then incubated for 1 h at room temperature with a 1:5 000 dilution of anti-rabbit/horseradish peroxidase or anti-mouse/horseradish peroxidase (Santa Cruz Biotechnology) and developed with the Chemiluminescence Plus Western Blot Analysis kit (Santa Cruz Biotechnology) [51, 61].

Real-time PCR

Total RNA was isolated with TRIzol reagent (Invitrogen) according to the manufacturer's instructions. Reverse transcription-PCR was performed as described previously [56, 62]. *p21* primer: 5′-AGTATGCCGTCGTCTGTTCG-3′ and 5′-GAGTGCAAGACAGCGACAAG-3′. For the glyceraldehyde-3-phosphate dehydrogenase gene (used as the internal control), the 5′-ACCACAGTCCATGCCATCAC-3′ and 5′-TTCACCACCCTGTTGCTGTA-3′ oligonucleotides were used. The PCR conditions were 25 cycles at 94 °C for 30 s, 55 °C for 30 s and 72 °C for 45 s.

Co-IP assay

Co-IP was performed as described previously [61, 63]. Briefly, cell extracts were first precleared with 25 μl of protein A-agarose (50% v/v). The supernatants were immunoprecipitated with 2 μg of anti-phosphoserine, anti-Klf5, anti-HDAC2 or anti-RARα antibodies for 1 h at 4 °C, followed by incubation with protein A-agarose overnight at 4 °C. Protein A-agarose-antigen-antibody complexes were collected by centrifugation at 12 000 rpm for 60 s at 4 °C. The pellets were washed five times with 1 ml IPH buffer (50 mM Tris-HCl, pH 8.0, 150 mM NaCl, 5 mM EDTA, 0.5% Nonidet P-40, 0.1 mM PMSF), for 20 min each time at 4 °C. Bound proteins were resolved by SDS-PAGE, followed by western blotting with the anti-Klf5, anti-RARα or anti-HDAC2 antibodies. The experiments were replicated three times at least.

ChIP assay

VSMCs at 80% confluence were crosslinked with 1% formaldehyde for 10 min, lysed as described above, and sonicated 5-10 times each for 10 s at 4 °C to reduce the average DNA length to 0.4-0.5 kb. The samples were diluted 10-fold and then precleared with protein A-agarose/salmon sperm DNA for 30 min at 4 °C followed by an overnight incubation at 4 °C with 1:500 anti-Klf5, 1:500 anti-RARα or 1:500 anti-mouse IgG (as a negative control). The immune complexes were precipitated with protein A-agarose for 1 h. After reversal of crosslinking, the genomic region of the *p21* flanking the potential Klf5-binding sites was amplified by PCR with the following primer pairs: 5′-TTCATAGATGTGCGTGGCTC-3′ (sense) and 5′-TTAACTCGGGCACTGTAGCA-3′ (antisense); the potential RARα-binding sites were amplified by PCR with the following primer pairs: 5′-GCCCTGAACTCCAAATACCA-3′ (sense) and 5′-CCATCTCTCCAGCCCTCTAA-3′ (antisense) [61, 64].

Oligo pull-down assay

The oligonucleotides containing biotin on the 5′-end of the each strand were used. The sequences of these oligonucleotides are as follows: the Klf5-binding site, biotin-5′-GGCGGGAGG GGGCGGGGTCGGGAGNGGGGGCGGGGCCAGGCCGAT g-3′ (forward), biotin-5′-CATCGGCCTGGCCCCGCCCCCNC TCCCGACCCCGCCCCCTCCCGCCG-3′ (reverse); the RARα-binding site 3, biotin-5′-GCATGCTGTCTTCTGCAGAGGTGA GAGGCAGGGAGACCCGGCTG-3′ (forward), biotin-5′-CAGC CGGGTCTCCCTGCCTCTCACCTCTGCAGAAGACAGCAT-GC-3′ (reverse). Each pair of oligonucleotides was annealed following standard protocols. VSMCs treated with or without Am80 for 2 h were lysed in lysis buffer (50 mM Tris-HCl, pH7.4, 150 mM NaCl, 1 mM EDTA, and 0.1% NP-40) containing protease inhibitors. Whole-cell extracts (100 μg) were precleared with ImmunoPure streptavidin-agarose beads (20 μl/sample, Promega) for 1 h at 4 °C. After centrifugation for 2 min at 12 000 rpm, the supernatant was incubated with 100 pmol of biotinylated double-stranded oligonucleotides and 10 μg of poly (dI-dC)·poly (dI-dC) overnight at 4 °C with gentle rocking. Then 30 μl of streptavidin-agarose beads was added, followed by further 1 h of incubation at 4 °C. The protein-DNA-streptavidin-agarose complex was washed four times with lysis buffer, separated on a 10% SDS-PAGE, and subjected to western blotting with different antibodies [61].

Site-directed mutagenesis of the TCE element of p21 promoter

Site-directed mutation of the TCE or RARE element of *p21* promoter was carried out by PCR using oligonucleotide primers that contain a base substitution at the TCE or RARE element. The reactions were carried out using a QuikChange site-directed mutagenesis kit (Stratagene). The introduced mutation was verified by DNA sequence analysis. Site-directed mutagenesis of RARE and TCE of *p21* promoter were RARE (5′-CAAAGG**T**GAAGTCCA-G**G**GGAGGTCAG-3′ to 5′-CAAAGG**C**GAAGTCCAG**A**GGAG-GTCAG-3′) and TCE (5′-G**T**GGGAATAGAGGTGATATTG**T**GG GGCTTTTCTGG••••••AG**T**GGGTCAGCG-3′ to 5′-G**G**GGGAAT AGAGGTGATATTG**G**GGGGCTTTTCTGG••••••AG**G**GGGTCA GCG-3′).

Protein phosphatase digestion

Immunoprecipitated fractions and DNA crosslinked protein fractions were incubated with or without calf intestinal alkaline phosphatase (Amersham Biosciences) at 37 °C for 1 h. The protein was separated on 12% SDS polyacrylamide gels and transferred onto nitrocellulose membrane for the indicated experiments.

Balloon injury model and drug treatment

Animal housing and procedures were approved by the local Animal Care and Use Committee at Hebei Medical University. The animals were anesthetized with urethane (600 mg/kg) intraperitoneally. The thoracic-abdominal artery was de-endothelialized, as described previously. In brief, the catheter was advanced from the left common carotid artery down to the level of the renal arteries three times with a 2-F (60 cm) Fogarty catheter (Baxter, McGaw Park, IL, USA). To attain a constant degree of vessel wall injury for each of the animals, we kept the diameter of the balloon and the resistance during withdrawal constant and the same for each of the animals [65]. A single operator performed all of the procedures. Am80 (1 mg/kg/day) was administered orally beginning 1 day before balloon injury and continuing for 3 or 14 days

thereafter. On hour 3 and day 14 after injury and administration of drugs orally, the animals were sacrificed with an overdose of pentobarbital (200 mg/kg), and the thoracic-abdominal artery was collected for western blot or hematoxylin/eosin staining.

Morphology analysis

At 14 days after balloon injury, six cross-sections from the middle of each abdominal artery were stained with hematoxylin/eosin. The neointimal and medial areas were calculated using the Image-Pro Plus Analyzer version 5.1 software (Media Cybernetics, Inc., Silver Spring, MD, USA) in a blind manner [65]. For each section, six random, noncontiguous microscopic fields were examined.

Immunohistochemistry

For antigen retrieval, deparaffinized formalin-fixed sections were boiled for 10 min in 10 mM sodium citrate (pH 6) [66]. Primary antibody (PCNA at 1:100, p21 at 1:100 dilutions) was incubated overnight at 4 °C in 1% normal goat serum in phosphate-buffered saline.

MTT assay

The cell growth rates were evaluated by the tetrazolium dye-based MTT assay, as described previously [67]. In brief, 1×10^4 cells/well were seeded in triplicate onto 96-well plates in DMEM. After 24 h, the cells were treated according to the experimental design. After each treatment, the medium was removed and the cells were washed with phosphate-buffered saline. The MTT reagent was added at 2 mg/ml in Hank's buffer and incubated for 1 h until dark blue crystals could be seen in the cytoplasm under light microscopy. The crystals were dissolved in DMSO, and the absorbance was measured in a Thermo Fluroscan Ascent spectrometer at 570 nm with background subtraction at 650 nm. The results were expressed as the means of the absorbance relative to time 0 or the control ± S.E.

Flow cytometry

VSMCs were treated by Am80 for 48 h, harvested, and fixed by drop-wise addition of 3 vol of ice-cold 70% ethanol. After treatment with RNase A (Roche) at 10 mg/ml in PBS, cells were resuspended in 1 mg/ml propidium iodide (Sigma-Aldrich) in PBS and subjected to analysis (FACSort; BD) using CellQuest Pro 4.02 (BD) and ModFit 3.0 (Verity Software House) softwares [23].

Statistical analysis

All of the data are expressed as the means ± S.E.M. Differences between two groups were assessed using analysis of variance followed by a Student's *t*-test.

Acknowledgments

This work was supported by the National Natural Science Foundation of China (90919035, 30971457, 30871272) and the Hebei Natural Science Foundation of China (C2007000831, C2009001541).

References

1 Francis DJ, Parish CR, McGarry M, *et al.* Blockade of vascular smooth muscle cell proliferation and intimal thickening after balloon injury by the sulfated oligosaccharide PI-88: phosphomannopentaose sulfate directly binds FGF-2, blocks cellular signaling, and inhibits proliferation. *Circ Res* 2003; **92**:e70-77.

2 Dzau VJ, Braun-Dullaeus RC, Sedding DG. Vascular proliferation and atherosclerosis: new perspectives and therapeutic strategies. *Nat Med* 2002; **8**:1249-1256.

3 Suzuki T, Sawaki D, Aizawa K, *et al.* Kruppel-like factor 5 shows proliferation-specific roles in vascular remodeling, direct stimulation of cell growth, and inhibition of apoptosis. *J Biol Chem* 2009; **284**:9549-9557.

4 Kunieda T, Minamino T, Nishi J, *et al.* Angiotensin II induces premature senescence of vascular smooth muscle cells and accelerates the development of atherosclerosis via a p21-dependent pathway. *Circulation* 2006; **114**:953-960.

5 Weinberg WC, Denning MF. P21Waf1 control of epithelial cell cycle and cell fate. *Crit Rev Oral Biol Med* 2002; **13**:453-464.

6 Avkin S, Sevilya Z, Toube L, *et al.* p53 and p21 regulate error-prone DNA repair to yield a lower mutation load. *Mol Cell* 2006; **22**:407-413.

7 Mattiussi S, Turrini P, Testolin L, *et al.* p21(Waf1/Cip1/Sdi1) mediates shear stress-dependent antiapoptotic function. *Cardiovasc Res* 2004; **61**:693-704.

8 Condorelli G, Aycock, JK, Frati G, Napoli C. Mutated p21/WAF/CIP transgene overexpression reduces smooth muscle cell proliferation, macrophage deposition, oxidation-sensitive mechanisms, and restenosis in hypercholesterolemic apolipoprotein E knockout mice. *FASEB J* 2001; **15**:2162-2170.

9 Olive M, Mellad JA, Beltran LE, *et al.* p21Cip1 modulates arterial wound repair through the stromal cell-derived factor-1/CXCR4 axis in mice. *J Clin Invest* 2008; **118**:2050-2061.

10 Otterbein LE, Zuckerbraun BS, Haga M, *et al.* Carbon monoxide suppresses arteriosclerotic lesions associated with chronic graft rejection and with balloon injury. *Nat Med* 2003; **9**:183-190.

11 Adimoolam S, Lin CX, Ford JM. The p53-regulated cyclin-dependent kinase inhibitor, p21 (cip1, waf1, sdi1), is not required for global genomic and transcription-coupled nucleotide excision repair of UV-induced DNA photoproducts. *J Biol Chem* 2001; **276**:25813-25822.

12 Agrawal S, Agarwal ML, Chatterjee-Kishore M, Stark GR, Chisolm GM. Stat1-dependent, p53-independent expression of p21(waf1) modulates oxysterol-induced apoptosis. *Mol Cell Biol* 2002; **22**:1981-1992.

13 Luo P, Lin M, Lin M, *et al.* Function of retinoid acid receptor alpha and p21 in all-trans-retinoic acid-induced acute T-lymphoblastic leukemia apoptosis. *Leuk Lymphoma* 2009; **50**:1183-1189.

14 Tanaka T, Suh KS, Lo AM, De Luca LM. p21WAF1/CIP1 is a common transcriptional target of retinoid receptors: pleiotropic regulatory mechanism through retinoic acid receptor (RAR)/retinoid X receptor (RXR) heterodimer and RXR/RXR homodimer. *J Biol Chem* 2007; **282**:29987-29997.

15 Narla G, Kremer-Tal S, Matsumoto N, *et al. In vivo* regulation of p21 by the Kruppel-like factor 6 tumor-suppressor gene in mouse liver and human hepatocellular carcinoma. *Oncogene* 2007; **26**:4428-4434.

16 Yoshida T, Kaestner KH, Owens GK. Conditional deletion of Kruppel-like factor 4 delays downregulation of smooth muscle cell differentiation markers but accelerates neointimal formation following vascular injury. *Circ Res* 2008; **102**:1548-1557.
17 Ghaleb AM, Nandan MO, Chanchevalap S, *et al.* Kruppel-like factors 4 and 5: the yin and yang regulators of cellular proliferation. *Cell Res* 2005; **15**:92-96.
18 Sue YM, Chung CP, Lin H, *et al.* PPARdelta-mediated p21/p27 induction via increased CREB-binding protein nuclear translocation in beraprost-induced antiproliferation of murine aortic smooth muscle cells. *Am J Physiol Cell Physiol* 2009; **297**:C321-C329.
19 Mottet D, Pirotte S, Lamour V, *et al*. HDAC4 represses p21(WAF1/Cip1) expression in human cancer cells through a Sp1-dependent, p53-independent mechanism. *Oncogene* 2009; **28**:243-256.
20 Kim JK, Esteve PO, Jacobsen SE, Pradhan S. UHRF1 binds G9a and participates in p21 transcriptional regulation in mammalian cells. *Nucleic Acids Res* 2009; **37**:493-505.
21 Bond M, Sala-Newby GB, Wu YJ, Newby AC. Biphasic effect of p21Cip1 on smooth muscle cell proliferation: role of PI 3-kinase and Skp2-mediated degradation. *Cardiovasc Res* 2006; **69**:198-206.
22 Zhang WQ, Geiman DE, Shields JM, *et al*. The Gut-enriched krüppel-like factor (krüppel-like factor 4) mediates the transactivating effect of p53 on the p21WAF1/Cip1 promoter. *J Biol Chem* 2000; **275**:18391-18398.
23 He M, Han M, Zheng B, Shu YN, Wen JK. Angiotensin II stimulates KLF5 phosphorylation and its interaction with c-Jun leading to suppression of p21 expression in vascular smooth muscle cells. *J Biochem* 2009; **146**:683-691.
24 Wassmann S, Wassmann K, Jung A *et al.* Induction of p53 by GKLF is essential for inhibition of proliferation of vascular smooth muscle cells. *J Mol Cell Cardiol* 2007; **43**:301-307.
25 Zhang XH, Zheng B, Han M, Miao SB, Wen JK. Synthetic retinoid Am80 inhibits interaction of KLF5 with RAR alpha through inducing KLF5 dephosphorylation mediated by the PI3K/Akt signaling in vascular smooth muscle cells. *FEBS Lett* 2009; **583**:1231-1236.
26 Liu R, Zheng HQ, Zhou Z, Dong JT, Chen C. KLF5 promotes breast cell survival partially through fibroblast growth factor-binding protein 1-pERK-mediated dual specificity MKP-1 protein phosphorylation and stabilization. *J Biol Chem* 2009; **284**:16791-16798.
27 Miano JM, Topouzis S, Majesky MW, Olson EN. Retinoid receptor expression and all-trans retinoic acid-mediated growth inhibition in vascular smooth muscle cells. *Circulation* 1996; **93**:1886-1895.
28 Miano JM, Kelly LA, Artacho CA, *et al.* all-Trans-retinoic acid reduces neointimal formation and promotes favorable geometric remodeling of the rat carotid artery after balloon withdrawal injury. *Circulation* 1998; **98**:1219-1227.
29 Axel DI, Frigge A, Dittmann J, *et al.* All-trans retinoic acid regulates proliferation, migration, differentiation, and extracellular matrix turnover of human arterial smooth muscle cells. *Cardiovas Res* 2001; **49**:851-862.
30 Wiegman PJ, Barry WL, McPherson JA, *et al*. All-trans-retinoic acid limits restenosis after balloon angioplasty in the focally atherosclerotic rabbit: a favorable effect on vessel remodeling. *Arterioscler Thromb Vasc Biol* 2000; **20**:89-95.
31 Herdeg C, Oberhoff M, Baumbach A, *et al.* Effects of local all-trans-retinoic acid delivery on experimental atherosclerosis in the rabbit carotid artery. *Cardiovasc Res* 2003; **57**:544-553.
32 Germain P, Iyer J, Zechel C, Gronemeyer H. Co-regulator recruitment and the mechanism of retinoic acid receptor synergy. *Nature* 2002; **415**:187-192.
33 Charoensit P, Kawakami S, Higuchi Y, Yamashita F, Hashida M. Enhanced growth inhibition of metastatic lung tumors by intravenous injection of ATRA-cationic liposome/IL-12 pDNA complexes in mice. *Cancer Gene Ther* 2010; **17**:512-522.
34 Fujiu K, Manabe I, Ishihara A, *et al.* Synthetic retinoid Am80 suppresses smooth muscle phenotypic modulation and instent neointima formation by inhibiting KLF5. *Circ Res* 2005; **97**:1132-1141.
35 Adenuga D, Rahman I. Protein kinase CK2-mediated phosphorylation of HDAC2 regulates co-repressor formation, deacetylase activity and acetylation of HDAC2 by cigarette smoke and aldehydes. *Arch Biochem Biophys* 2010; **498**:62-73.
36 Tsai SC, Seto E. Regulation of histone deacetylase 2 by protein kinase CK2. *J Biol Chem* 2002; **277**:31826-31833.
37 Miyamoto S, Suzuki T, Muto S, *et al.* Positive and negative regulation of the cardiovascular transcription factor KLF5 by p300 and the oncogenic regulator SET through interaction and acetylation on the DNA-binding domain. *Mol Cell Biol* 2003; **23**:8528-8541.
38 Guo P, Zhao KW, Dong XY, Sun X, Dong JT. Acetylation of KLF5 alters the assembly of p15 transcription factors in transforming growth factor-beta-mediated induction in epithelial cells. *J Biol Chem* 2009; **284**:18184-18193.
39 Eberharter A, Becker PB. Histone acetylation: a switch between repressive and permissive chromatin. Second in review series on chromatin dynamics. *EMBO Rep* 2002; **3**:224-229.
40 Marks PA, Richon VM, Miller T, *et al*. Histone deacetylase inhibitors. *Adv Cancer Res* 2004; **91**:137-168.
41 Zimmermann S, Kiefer F, Prudenziati M, *et al*. Reduced body size and decreased intestinal tumor rates in HDAC2-mutant mice. *Cancer Res* 2007; **67**:9047-9054.
42 Rössig L, Urbich C, Brühl T, *et al.* Histone deacetylase activity is essential for the expression of HoxA9 and for endothelial commitment of progenitor cells. *J Exp Med* 2005; **201**:1825-1835.
43 Peinado H, Ballestar E, Esteller M, *et al*. Snail mediates E-cadherin repression by the recruitment of the Sin3A/histone deacetylase 1 (HDAC1)/HDAC2 complex. *Mol Cell Biol* 2004; **24**:306-319.
44 Li J, Wang J, Wang J, *et al*. Both corepressor proteins SMRT and N-CoR exist in large protein complexes containing HDAC3.*EMBO J* 2000; **19**:4342-4350.
45 Meng F, Han M, Zheng B, *et al*. All-trans retinoic acid increases KLF4 acetylation by inducing HDAC2 phosphorylation and its dissociation from KLF4 in vascular smooth muscle cells. *Biochem Biophys Res Commun* 2009; **387**:13-18.
46 Yoshida T, Gan Q, Owens GK. Krüppel-like factor 4, Elk-1,

and histone deacetylases cooperatively suppress smooth muscle cell differentiation markers in response to oxidized phospholipids. *Am J Physiol Cell Physiol* 2008; **295**:C1175-C1182.

47 van Wely KH, Molijn AC, Buijs A, *et al.* The MN1 oncoprotein synergizes with coactivators RAC3 and p300 in RAR-RXR-mediated transcription. *Oncogene* 2003; **22**:699-709.

48 Lin YC, Lin JH, Chou CW, *et al.* Statins increase p21 through inhibition of histone deacetylase activity and release of promoter-associated HDAC1/2. *Cancer Res* 2008; **68**:2375-2383.

49 Delarue FL, Adnane J, Joshi B, *et al.* Farnesyltransferase and geranylgeranyltransferase I inhibitors upregulate RhoB expression by HDAC1 dissociation, HAT association and histone acetylation of the RhoB promoter. *Oncogene* 2007; **26**:633-640.

50 Ryu H, Lee J, Olofsson BA, *et al.* Histone deacetylase inhibitors prevent oxidative neuronal death independent of expanded polyglutamine repeats via an Sp1-dependent pathway. *Proc Natl Acad Sci USA* 2003; **100**:4281-4286.

51 Zheng B, Han M, Bernier M, *et al.* Kruppel-like factor 4 inhibits proliferation by platelet-derived growth factor receptor beta-mediated, not by retinoic acid receptor alpha-mediated, phosphatidylinositol 3-kinase and ERK signaling in vascular smooth muscle cells. *J Biol Chem* 2009; **284**:22773-22785.

52 Chen LF, Williams SA, Mu Y, *et al.* NF-kappaB RelA phosphorylation regulates RelA acetylation. *Mol Cell Biol* 2005; **25**:7966-7975.

53 Elmazar MM, Nau H. Potentiation of the teratogenic effects induced by coadministration of retinoic acid or phytanic acid/phytol with synthetic retinoid receptor ligands. *Arch Toxicol* 2004; **78**:660-668.

54 Dong LH, Wen JK, Liu G, *et al.* Blockade of the Ras-extracellular signal-regulated kinase 1/2 pathway is involved in smooth muscle 22 alpha-mediated suppression of vascular smooth muscle cell proliferation and neointima hyperplasia. *Arterioscler Thromb Vasc Biol* 2010; **30**:683-691.

55 Nofsinger RR, Li P, Hong SH, *et al.* SMRT repression of nuclear receptors controls the adipogenic set point and metabolic homeostasis. *Proc Natl Acad Sci USA* 2008; **105**:20021-20026.

56 Chanchevalap S, Nandan MO, McConnell BB, *et al.* Kruppel-like factor 5 is an important mediator for lipopolysaccharide-induced proinflammatory response in intestinal epithelial cells. *Nucleic Acids Res* 2006; **34**:1216-1223.

57 Choi YB, Ko JK, Shin J. The transcriptional corepressor, PELP1, recruits HDAC2 and masks histones using two separate domains. *J Biol Chem* 2004; **279**:50930-50941.

58 Flinterman MB, Mymryk JS, Klanrit P, *et al.* p400 function is required for the adenovirus E1A-mediated suppression of EGFR and tumour cell killing. *Oncogene* 2007; **26**:6863-6874.

59 Macleod KF, Sherry N, Hannon G, *et al.* p53-dependent and independent expression of p21 during cell growth, differentiation, and DNA damage. *Genes Dev* 1995; **9**:935-944.

60 Zheng B, Han M, Wen JK, Zhang R. Human heart LIM protein activates atrial-natriuretic-factor gene expression by interacting with the cardiac-restricted transcription factor Nkx2.5. *Biochem J* 2008; **409**:683-690.

61 Li HX, Han M, Bernier M, *et al.* Kruppel-like factor 4 promotes differentiation by transforming growth factor-beta receptor-mediated Smad and p38 MAPK signaling in vascular smooth muscle cells. *J Biol Chem* 2010; **285**:17846-17856.

62 Han M, Wen JK, Zheng B, Cheng Y, Zhang C. Serum deprivation results in redifferentiation of human umbilical vascular smooth muscle cells. *Am J Physiol Cell Physiol* 2006; **291**:C50-C58.

63 Zheng B, Wen JK, Han M. hhLIM is a novel F-actin binding protein involved in actin cytoskeleton remodeling. *FEBS J* 2008; **275**:1568-1578.

64 Han M, Li AY, Meng F, *et al.* Synergistic co-operation of signal transducer and activator of transcription 5B with activator protein 1 in angiotensin II-induced angiotensinogen gene activation in vascular smooth muscle cells. *FEBS J* 2009; **276**:1720-1728.

65 Liu B, Han M, Wen JK. Acetylbritannilactone inhibits neointimal hyperplasia after balloon injury of rat artery by suppressing nuclear factor-{kappa}B activation. *J Pharmacol Exp Ther* 2008; **324**:292-298.

66 Sun SG, Zheng B, Han M, *et al*. miR-146a and Krüppel-like factor 4 form a feedback loop to participate in vascular smooth muscle cell proliferation. *EMBO Rep* 2011; **12**:56-62.

67 Wu L, Li X, Li Y, *et al.* Proliferative inhibition of danxiongfang and its active ingredients on rat vascular smooth muscle cell and protective effect on the VSMC damage induced by hydrogen peroxide. *J Ethnopharmacol* 2009; **126**:197-206.

(**Supplementary information** is linked to the online version of the paper on the *Cell Research* website.)